

THESIS

INFLUENCE OF GEOCHEMICAL PROCESSES ON GEOTECHNICAL STABILITY
OF TAILINGS STORAGE FACILITIES

Submitted by

Heath Marie Orcutt

Department of Civil and Environmental Engineering

In partial fulfillment of the requirements

For the Degree of Master of Science

Colorado State University

Fort Collins, Colorado

Summer 2023

Master's Committee:

Advisor: Joseph Scalia IV

Co-Advisor: Christopher Bareither

John Ridley

Copyright by Heath Marie Orcutt 2023

All Rights Reserved

ABSTRACT

INFLUENCE OF GEOCHEMICAL PROCESSES ON GEOTECHNICAL STABILITY OF TAILINGS STORAGE FACILITIES

Incorporation of geochemically induced material changes and weathering patterns into geotechnical design and long-term stability analyses of tailings storage facilities has yet to be implemented widely or consistently. Tailings are deposited in disequilibrium with the surrounding environment and must undergo physical, chemical, and biological weathering to reach their most stable form. As a result, the geotechnical properties of the tailings (i.e., particle size, water retention capacity, shear strength, etc.) change over time. Herein, an in-depth review of published literature is provided, ranging across multiple disciplines (geochemistry, geotechnical engineering, hydrogeology, environmental engineering, mining engineering), and focusing on studies that document or allude to material property changes of weathered sulfidic base metal tailings. Synthesized visual aids are provided as a framework for beginning interdisciplinary conversation that couples geochemistry and geotechnical engineering. By drawing attention to potential geochemically induced failure modes, I hope to draw connections between geochemistry and geotechnical engineering that are fundamental to developing robust designs and advanced monitoring plans that ensure long-term tailings storage facility stability. A “proof of concept” laboratory design is presented which analyzes changes to the physical material properties (compressibility, permeability, and shear strength) of saturated fine-synthetic tailings mixed with calcite at

different pH values. Overall, this report seeks to lay the foundation for future study and advance communication between experts.

ACKNOWLEDGMENTS

I would like to thank the following individuals for their guidance and support in the completion of this document and for playing a role in my success. My research advisors, Joseph Scalia and Christopher Bareither, brought me to Colorado State University and introduced me to the world of tailings. I hope, through your education, that I can contribute to the betterment of the mining and tailings industry. To the several tailings professionals who discussed their work with me over Tailings and Mine Waste luncheons and Zoom calls, thank you for taking the time to answer my questions and provide me with direction in the generation of this report. Specifically, I would like to thank Oscar Benavente, Kelly Sexsmith, Hugh Davies, Sarah Doyle, Linda Figueroa, and John Ridley for their feedback on the geochemical conceptual model. Special credit is due to Jennifer Durocher for her advancement in this niche topic, albeit no direct affiliation is made with this work.

Personally, I would like to thank the support network of family and friends that hides behind each body of work. To my family, your role in my success never goes unnoticed or unappreciated. Thank you for your unrelenting love – it is the best thing I’ve got. To the “geo-group”, thank you for never failing to keep things interesting. You all are some of the most thoughtful, goofy, and passionate people I’ve had the pleasure of knowing and I look forward to our reunions at Tailings and Mine Waste every year for the rest of time, forever. As Garret Martin would say, “lightning in a bottle...”. Lastly, thank you to my community in Fort Collins, life here would not have been nearly as magical without you.

TABLE OF CONTENTS

ABSTRACT.....	ii
ACKNOWLEDGMENTS.....	iv
LIST OF TABLES	viii
LIST OF FIGURES.....	ix
CHAPTER 1. INTRODUCTION	1
CHAPTER 2. GEOCHEMISTRY AS FUNDAMENTAL TO TAILINGS GEOTECHNICS	4
2.1. Introduction.....	4
2.2. TSF Geochemical Conceptual Model	6
2.2.1. Physical, Chemical, and Biological Weathering.....	8
2.2.2. Primary and Secondary Minerals	10
2.3. Potential Weathering Processes.....	11
2.3.1. Primary Mineral Alteration from Redox Processes.....	12
2.3.1.a. Alteration of Microstructure.....	13
2.3.1.b. Generation & Migration of Fines.....	14
2.3.1.c. Cementation of Tailings.....	16
2.3.1.d. Clogging of Drainage.....	18
2.3.2. Primary Mineral Alteration from Acid-Neutralizing Reactions.....	20
2.3.2.a. Dissolution of Carbonates	20
2.3.2.b. Precipitation of Carbonates	21
2.3.2.c. Weathering of Silicates to Clays.....	22

2.3.3.	Hardpan Formation	24
2.3.3.a.	Gypsum Formation	25
2.3.3.b.	Creation of Low Permeability Zones	26
2.3.3.c.	Localized Cementation of Tailings	27
2.4.	Influence on Potential Failure Modes	28
2.4.1.	Flow-type Stability Failure Mode	29
2.4.2.	Water Management Failure Mode	31
2.4.3.	Internal Erosion and Piping Failure Mode	34
2.4.4.	Foundational Failure Mode	36
2.5.	Monitoring Potential Failure Modes	39
2.5.1.	Sensitivity Analyses	40
2.5.2.	Monitoring Tools	40
2.5.2.a.	Monitoring Flow-Type Stability Failure Modes	40
2.5.2.b.	Monitoring Water Management Failure Modes	42
2.5.2.c.	Monitoring Internal Erosion and Piping Failure Modes	43
2.5.2.d.	Monitoring Foundational Failure Modes	44
CHAPTER 3. LABORATORY METHODS & PRELIMINARY RESULTS		47
3.1.	Objectives and Hypotheses	47
3.2.	Methods and Materials	48
3.3.	Data Analysis	51

3.4. Preliminary Results	53
CHAPTER 4. FUTURE WORK AND CONCLUSIONS.....	57
4.1. Questa Rock Pile Weathering and Stability Project.....	57
4.2. Remote Sensing.....	58
4.3. Future Field and Laboratory Methods.....	62
4.4. Microbial Technologies	63
4.5. Conclusion	63
REFERENCES.....	65
APPENDIX A. LABORATORY PHOTOS	82

LIST OF TABLES

Table 1: Summary of Fine Synthetic Tailings Geotechnical Characteristics. Unified Soil Classification System (USCS) soil type is lean clay (CL).....	49
Table 2: Summary of all column experiment inputs.....	51
Table 3: Summary of empirical parameters (Z, A, C, B, and D) for columns 1, 2, and 4...	53

LIST OF FIGURES

Figure 1: Geochemical conceptual model summarizing major geochemical processes occurring within a tailings storage facility that may alter physical material properties. Numbers denote different processes that may occur in a tailings storage facility comprised of sulfidic base metal tailings containing carbonates. Note, not all these processes will occur simultaneously. 7

Figure 2: Conceptual schematic of the influence of microbes on the rate of sulfide oxidation and subsequent outcomes. FeS₂ (pyrite) is oxidized to Fe²⁺ (ferrous iron), sulfate (SO₄²⁻), and acidity H⁺ both abiotically and biotically. Fe²⁺ is rapidly oxidized to Fe³⁺ via iron-oxidizing bacteria (gray ovals) which enhances the rate of sulfide oxidation and forms secondary iron oxy-hydroxides (FeOOH = ferrihydrite). The acid generated (H⁺) breaks down silicate minerals (Fsp = feldspar) into phyllosilicate minerals (clays) and sulfate (SO₄²⁻) reacts to form gypsum. 11

Figure 3: Process map breaking down major geochemical processes occurring within TSF. 12

Figure 4: Conceptual schematic of the alteration of rough, crystalline primary minerals such as pyrite (Py) and pyrrhotite (Po) to smooth, amorphous secondary minerals (e.g., ferric hydroxide, Fe(OH)₃). 14

Figure 5: Light cementitious bridges of secondary Fe-minerals forming between particles. 17

Figure 6: Clogging of drainpipes due to secondary mineral precipitation. Fe^{2+} , aqueous ferrous iron, shown precipitating as Fe^{3+} under oxidizing conditions. Calcite (CaCO_3) precipitation under atmospheric partial pressure of CO_2 and amorphous silica mineral formation (SiO_2)..... 19

Figure 7: Dissolution of soluble mineral phase (e.g., calcite, Cal and dolomite, Dol) leading to dissolved calcium and carbonate ions in solution. 21

Figure 8: Precipitation of soluble mineral phase (e.g., calcite, CaCO_3) between tailings particles (quartz, Qtz). Reprecipitation occurs due to supersaturation of calcium (Ca^{2+}) and carbonate (CO_3^{2-}) and high partial pressure of CO_2 in the tailings reaching atmospheric equilibrium. 22

Figure 9: The breakdown of primary silicate minerals in embankment to secondary phyllosilicate clay layers via hydrolysis (interaction with H^+ and OH^-). Interface between embankment materials and atmosphere is delineated by the black line..... 23

Figure 10: Schematic of sulfide-induced heave occurring via gypsum formation from the reaction of calcium ions (Ca^{2+}) and sulfate ions (SO_4^{2-}) along discontinuity in bedrock. .. 26

Figure 11: Hardpan formation at interface between oxidized zone (orange) and transition zone (yellow). Hardpans limits oxygen ingress (sulfide oxidation) and evaporation (desiccation)..... 27

Figure 12: Potential flow-type stability failure mode due to cementation of embankment materials creating a brittle, stiff, and contractive material. Advanced weathering causes a buildup of pore water pressure and the development of a critical slip surface..... 30

Figure 13: Schematic of water management failure due to a series of weathering reactions. Failure includes hindered drainage, erosion due to overtopping, slope instability, increased liquefaction potential, and more..... 32

Figure 14: Schematic demonstrating internal erosion and piping failure mode accentuated by alteration of the soluble mineral phase and the buildup of pore water due to various geochemical processes..... 35

Figure 15: Schematic demonstrating potential foundational failure modes via karstic bedrock dissolution, clay formation, and sulfate- induced heave via gypsum formation along discontinuities. Formation of critical slip surface under embankment shown in red. 37

Figure 16: Relationship between vertical displacement (mm) and elapsed time (hr) for columns 1, 2, and 4. 53

Figure 17: Relationship between final void ratio and effective stress (kPa) for columns 1, 2, and 4..... 54

Figure 18: Relationship between final void ratio and hydraulic conductivity (m/s) for columns 1, 2, and 4. 55

Figure 19: Results of laboratory mini vane shear for columns 1, 2, and 4..... 55

Figure 20: Results of remote-sensing imagery on the Goat Hill North rock pile showing visible goethite, hematite, jarosite, copiapite, and gypsum surface precipitation (Hauff et al., 2013)..... 60

Figure 21: Results of remote-sensing imagery on the Goat Hill North rock pile showing surficial clay formation from weathered silicates (Hauff et al., 2013). 60

CHAPTER 1. INTRODUCTION

Tailings are the waste solids left over from the separation of valuable minerals from uneconomic minerals. After mineral extraction and beneficiation, the residuals from mineral recovery are typically discharged as a slurry composed of sub-micrometer to sand-sized particles, chemicals, and process water into a tailings storage facility (TSF) (Wang et al., 2014). The resulting fine-grained material is termed tailings. After deposition, tailings undergo physical, chemical, and biological weathering towards equilibrium with the surrounding environment. As a result of weathering processes, the geotechnical properties (i.e., shear strength, hydraulic conductivity, volume change) of the tailings change over time. Previous TSF failures and *in-situ* observations of tailings material property changes have yielded the question: how well do we, as an industry, understand the entire lifespan (25, 50, 100+ years) of the material we are working with and, specifically, how do the geotechnical parameters used in design change over time due to geochemical processes and biological activity? Our current design approaches generally do not incorporate the long-term role of geochemistry on TSF geotechnics.

Limited information on this topic has been shared in the peer-reviewed literature. There are currently no laboratory procedures which quantify the impact of weathering on the geotechnical parameters of slurry-like materials. Available procedures such as the humidity cell test (ASTM D5744) or hydraulic conductivity compatibility tests (e.g., ASTM D5084, D6766) have yet to be considered in terms of both geochemical and geotechnical significance of tailings. Even if these methods were designed to do so, accelerated weathering laboratory tests are unlikely to reproduce the complex tailings fabric that is naturally formed over time due to a series of dissolution-precipitation, oxidation-reduction, and acid-neutralization

reactions within a microbially mediated and kinetically controlled system. Therefore, the best analogs for operating facilities are likely to be those which have been closed for 25-50+ years and in which weathering patterns and profiles can be observed and analyzed, as was done for the Questa Rock Pile Weathering and Stability Project (Robertson, 2001; Shaw et al., 2002; URS Corporation, 2001). Overall, increased sharing of information, research, and the development of better field and/or laboratory procedures are all pathways to enhance our collective understanding of geochemical processes and how they influence the geotechnical stability of TSFs.

Herein, I seek to review the published literature across disciplines regarding the geochemical weathering of sulfidic base metal tailings, with an emphasis on studies that mention material property changes. I chose to focus on sulfidic tailings due to the tendency of these materials to generate acid rock drainage (ARD) and, ARD being the most understood and widely studied geochemical phenomenon, serves as a robust starting point for diving deeper into how geochemical processes go beyond impacts to water quality. By highlighting our understanding of geochemical processes that may occur within tailings and making direct connections to geotechnical properties and potential failure modes, I hope to explain the importance of these geochemical processes and geotechnical alterations to geotechnical engineers and geochemists alike. This thesis builds upon the literature review and summaries geochemical processes relevant to dam stability developed by Durocher (2017, 2022); however, there is no direct affiliation with this work. The use of synthesized visual aids is intended as a framework for interdisciplinary conversation. By bringing attention to how geochemistry may contribute to potential geotechnical failure modes, I hope to draw connections between geochemistry and geotechnical engineering that are fundamental to

developing advanced monitoring plans and robust designs that ensure long-term TSF stability.

My goal from this work is to highlight the need for future research and interdisciplinary collaboration to advance the current state of practice. Chapter 2 provides a review and synthesis of geochemical processes and the potential influence of these processes on geotechnical parameters, which is then carried forward towards possible effect on geotechnical failure modes and potential monitoring tools. Chapter 3 provides a “proof-of-concept” laboratory test design to broadly assess the potential for geotechnically impactful geochemical processes and provides results of preliminary laboratory analyses. Finally, Chapter 4 provides recommended next steps to advance the integration of tailings geochemistry and geotechnical engineering.

CHAPTER 2. GEOCHEMISTRY AS FUNDAMENTAL TO TAILINGS GEOTECHNICS

2.1. Introduction

Tailings are the waste solids left over from the separation of valuable minerals from economically invaluable minerals. After mineral extraction and beneficiation, the residuals from mineral recovery are discharged as slurry composed of waste minerals that have been ground to form sub-micrometer to sand-sized particles, chemicals, and process water (Wang et al., 2014). In most cases, conventional management of tailings occurs by hydraulic discharge into an impoundment or ‘tailings storage facility’ (TSF) where solids separate from water under gravity, and then slowly compress under self-weight over decades or centuries (Vick, 1990; Blight, 2010; Cambridge, 2017). Within TSFs, tailings are exposed to natural weathering processes via interactions with oxygen, water, and biological activity and, like any natural system, must undergo physical, chemical, and biological weathering to reach equilibrium with the environment. Often this involves the weathering of primary minerals (e.g., pyrite, feldspar, biotite, etc.) to secondary minerals (e.g., gypsum, jarosite, goethite, etc.) that may alter shear strength, particle size, permeability, and volume change characteristics (Durocher et al., 2022).

Although often termed tailings ‘storage’ facilities, these facilities are not temporary, and cannot be discarded at the end of useful life. The aim of TSFs is to ensure deposited materials achieve both geotechnical and geochemical stability in the long-term. Closure of tailings requires ensuring acceptably low risks for hundreds or thousands of years (Blight, 2010). As an industry, we have yet to adopt tailings management standards which take into consideration the long-term geochemical alteration of tailings and subsequent material

property changes over time. This is due, in part, to the relative newness of modern tailings storage facilities compared to the time required for some geochemical processes to occur at a magnitude sufficient to be obviously impactful. In addition, ore processing techniques have advanced, allowing for greater mineral extraction, and generating finer particles that are more susceptible to weathering. Warming climates will also increase the rate of physical, chemical, and biological weathering through more intense wetting/drying cycles, hotter temperatures promoting microbial activity, etc. Considering that TSFs must be monitored into perpetuity, adjusting our minds to timeframes of 50, 100, 1000 years into the future is an important step in incorporating short- and long-term weathering patterns into tailings design.

Herein I draw upon published literature in various fields (microbiology, geosciences, environmental engineering, geotechnical engineering) to summarize the current state of (shared) knowledge on the role of geochemical processes on tailings geotechnics with a focus on sulfidic base-metal tailings. Sulfide minerals are often found in mining environments as pyrite (FeS_2), pyrrhotite ($\text{Fe}_{(1-x)}\text{S}$), galena (PbS), chalcopyrite (CuFeS_2), and more. Sulfide oxidation is a chemical weathering process that transforms primary sulfide minerals into sulfate (SO_4^{2-}), acidity (H^+), and other dissolved metals (e.g., Fe^{2+}); a process classically known as acid-rock drainage (ARD) (Evangelou and Zhang, 1995; Nordstrom et al., 2015; Singer and Stumm, 1970). Ferrous iron (Fe^{2+}) then undergoes chemical and/or biological oxidation to ferric iron (Fe^{3+}) which, upon supersaturation in the pore water, begins to react with nutrients (K^+ , Na^+ , Ca^{2+}), water, sulfates, and hydroxide to form more stable, secondary metal(loid)-oxyhydroxides and metal-sulfate compounds (McGregor et al., 1998). In addition, the acidity that is released from sulfide oxidation may

be capable of weathering primary silicate minerals and soluble minerals such as biotite, feldspars, calcite, dolomite, etc. (Balkenhol et al., 2001; Durocher et al., 2022)

This review highlights the need for future research, evaluation of existing data with a weathering mindset, and the sharing of unpublished studies to advance the current state of practice for incorporating geochemical weathering patterns into geotechnical design of mine waste structures.

2.2. TSF Geochemical Conceptual Model

A conceptual cross section highlighting geochemical processes and the resultant potential impact on geotechnical parameters is shown in Figure 1. The TSF is formed by an embankment constructed to contain the slurry-deposited tailings. Tailings are discharged from the embankment such that hydraulic sorting occurs as particle velocities decrease away from the containment structure, with coarse particles (sand sized) settling first. The impounded ‘slimes’ (fines) are slow to release water and gain strength. Unlike water dams, TSF embankments are maintained in an unsaturated condition to assist in the draining of pore fluids via consolidation, facilitate incremental construction, and minimize the potential for static or dynamic liquefaction. Seepage control drains and seepage return pipes are used to collect seepage that does occur, reducing pore water pressures.

Figure 1 is intended to summarize multiple geochemical processes that occur throughout the lifetime of a TSF, independent of site-specific mineralogy and/or climate. A generalized carbonate-bearing, sulfidic ore tailings is presented. I note that not all these processes will occur simultaneously or at every facility. An upstream dam construction has been chosen due to the high frequency of legacy facilities built using this depositional method (Blight, 2010).

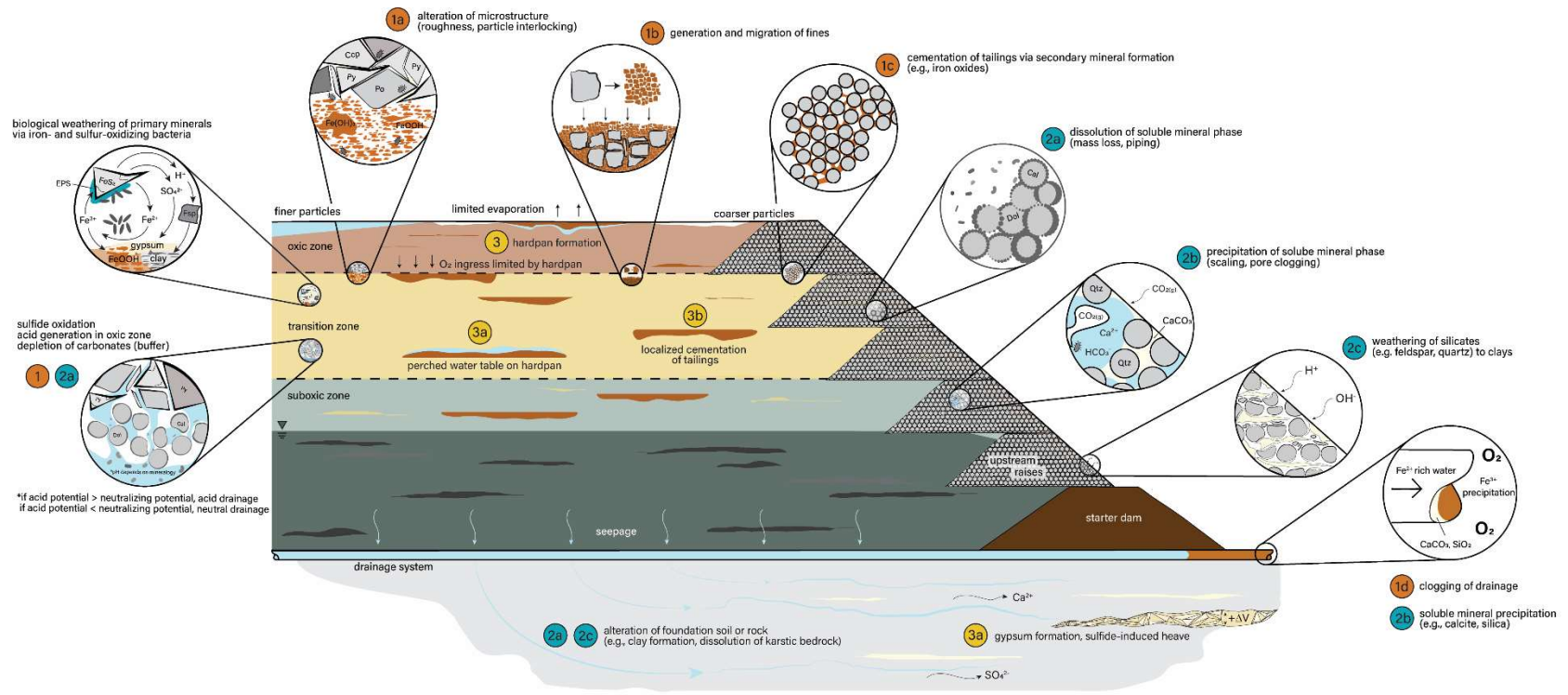


Figure 1: Geochemical conceptual model summarizing major geochemical processes occurring within a tailings storage facility that may alter physical material properties. Numbers denote different processes that may occur in a tailings storage facility comprised of sulfidic base metal tailings containing carbonates. Note, not all these processes will occur simultaneously, or will occur in every facility.

Figure 1 is divided into three zones: oxic zone, transition zone, and anoxic zone. The oxic zone is along the perimeter of the facility where oxygen ingress is the rate-limiting step of sulfide oxidation. The oxic zone typically consists of secondary minerals that form at higher oxidation-reduction (redox) states (i.e., more oxidized) and is typically orange in color from the high iron oxide and oxyhydroxide content (Blowes and Jambor, 1990; Durocher, 2017). The transition zone (green gray) underlies the oxic zone and consists of slightly weathered material due to the limited oxygen ingress with depth and increase in pH as carbonate minerals buffer acidic pore water generated in the oxic zone (Blowes et al., 1998; Durocher, 2017). The secondary minerals that form depend on pH, redox, temperature, microbial ecology, pressure, and pore water chemistry at the time of formation (Durocher et al., 2017). Underlying the oxic and transition zones is the anoxic zone (dark grey) that mainly consists of unweathered tailings. Sulfide oxidation in this zone is limited due to oxidant diffusion from the environment.

2.2.1. Physical, Chemical, and Biological Weathering

Like any natural terrestrial rock or soil, tailings experience physical, chemical, and biological weathering. The more stable a mineral, the slower the mineral weathers (Mitchell and Soga, 2005). For example, halite (or table salt) will dissolve rapidly in a glass of water, whereas quartz sand will remain intact for many years. Physical weathering often precedes chemical weathering and is responsible for decreasing particle size, increasing surface area, and increasing bulk volume (Mitchell and Soga, 2005). In tailings, physical weathering occurs primarily through grinding and crushing of ore; however, once the material is placed, physical weathering can continue via unloading, thermal expansion

and contraction, crystal growth (frost action), colloid plucking, and organic activity (Mitchell and Soga, 2005).

Chemical weathering processes include hydrolysis, chelation, cation exchange, oxidation-reduction, carbonation, and hydration (Mitchell and Soga, 2005). Examples related to the chemical weathering of tailings include oxidation of sulfides, dissolution of carbonates, gypsum formation, and cation exchange of clay minerals.

Biological weathering of tailings occurs primarily via microbial activity. Microbes are ubiquitous in mine waste and tailings (Schippers et al. 2010). The contribution of microbes to acid-generation and subsequent weathering of mine waste is also well established (Blowes et al., 1998; Nordstrom et al., 2015; Nordstrom and Southam, 1997). Figure 2 provides a conceptual schematic of how microbes influence the rate of sulfide oxidation in tailings. The cycle of Fe^{2+} to Fe^{3+} is shown as accelerated by microbial activity (gray ovals) because iron-oxidizing bacteria (e.g., *Acidithiobacillus ferrooxidans*) are known to be capable of accelerating the rate of iron oxidation by up to six orders of magnitude relative to the abiotic rate (Nordstrom, 2003; Singer and Stumm, 1970). Microbes also form extracellular polymeric substances (EPS), shown in blue, which enhance microbe-mineral contact (Flemming, 2011; Yi et al., 2021, 2023). The oxidation of pyrite (FeS_2) produces acidity (H^+) and sulfate (SO_4^{2-}), capable of accelerating the breakdown of other primary minerals (e.g., feldspar, Fsp), and forming secondary metal-sulfates (e.g., gypsum). Pyrrhotite is considered the most susceptible iron sulfide to microbial oxidation due to its higher surface reactivity (Blowes and Jambor, 1990).

2.2.2. *Primary and Secondary Minerals*

Understanding prevalent primary minerals in tailings provides a starting point for discussions of mineral transformations. Primary minerals are those originally present in the ore body and gangue mineral assemblages, and, in acid-generating ore deposits, typically consist of silicates (e.g., quartz, feldspars, micas, amphiboles), carbonates (e.g., calcite, dolomite-ankerite, siderite), and sulfides (e.g., pyrite, pyrrhotite, chalcopyrite) (Nordstrom et al., 2015). Secondary minerals are weathering products that form in mine wastes as a result of redox processes and acid-neutralizing reactions and include metal-oxides (e.g., hematite, Fe_2O_3), metal-oxyhydroxides (e.g., goethite, FeOOH), metal-sulfates (e.g., gypsum, $\text{CaSO}_4 \cdot 2\text{H}_2\text{O}$), metal-hydroxy-sulfates (e.g., jarosite, $\text{KFe}_3(\text{SO}_4)_2(\text{OH})_6$), and phyllosilicates (e.g., kaolinite, $\text{Al}_2\text{Si}_2\text{O}_5(\text{OH})_4$) (Durocher, 2023; Nordstrom et al., 2015). While most of these are examples of Fe-bearing minerals, the metal ion can be replaced by aluminum (Al^{3+}), calcium (Ca^{2+}), copper (Cu^{2+}), lead (Pb^{2+}), or barium (Ba^{2+}), depending on the environmental conditions present during formation (Durocher et al., 2017).

Silicates consist of essential nutrients needed for microbial activity (Na^+ , K^+ , Mg^{2+}) and secondary mineral formation (e.g., jarosite, $\text{KFe}_3(\text{SO}_4)_2(\text{OH})_6$) (McGregor et al., 1998). Silicates also break down into phyllosilicates (clay minerals). Sulfides are acid-generating. Carbonates, hydroxides, and silicates are acid-neutralizing, and the precipitation of secondary aluminum and ferric hydroxides can also raise pore water pH (Nordstrom et al., 2015). The ratio of acid-generating potential to acid-neutralizing potential is what ultimately governs seepage pore water chemistry (Blowes and Jambor, 1990; Nordstrom et al., 2015).

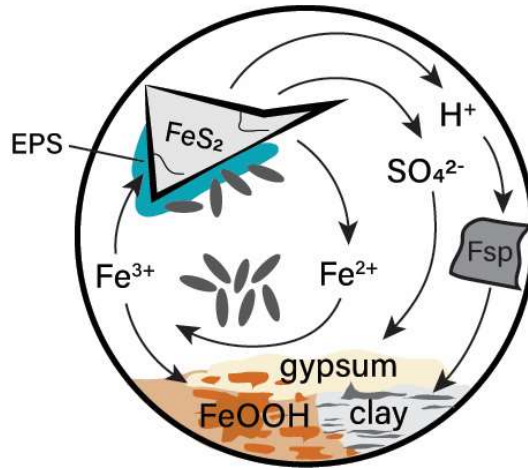


Figure 2: Conceptual schematic of the influence of microbes on the rate of sulfide oxidation and subsequent outcomes. FeS_2 (pyrite) is oxidized to Fe^{2+} (ferrous iron), sulfate (SO_4^{2-}), and acidity (H^+) both abiotically and biotically. Fe^{2+} is rapidly oxidized to Fe^{3+} via iron-oxidizing bacteria (gray ovals) which enhances the rate of sulfide oxidation and forms secondary iron oxyhydroxides (FeOOH = ferrihydrite). The acid generated (H^+) breaks down silicate minerals (Fsp = feldspar) into phyllosilicate minerals (clays) and sulfate (SO_4^{2-}) reacts to form gypsum.

2.3. Potential Weathering Processes

A summary of major geochemical weathering processes and the potential impact of these processes on geotechnical engineering parameters is provided in the following subsections. The sections align with and expand upon a framework established by Durocher et al., (2023) for consistency. The sections are as follows: (1) primary mineral alteration from redox processes; (2) primary mineral alteration from acid-neutralizing reactions; and (3) hardpan formation. Primary mineral alteration from redox processes includes sulfide oxidation and formation of secondary Fe-bearing mineral precipitates. Primary mineral alteration from acid-neutralizing reactions involves the dissolution and precipitation of carbonates and silicate minerals. Hardpan (thick, cemented layers of secondary mineral precipitates) and gypsum formation is shown amidst weathering of primary minerals and

soluble mineral alteration due to the need for the former to occur and generate the byproducts needed for hardpan and gypsum formation.

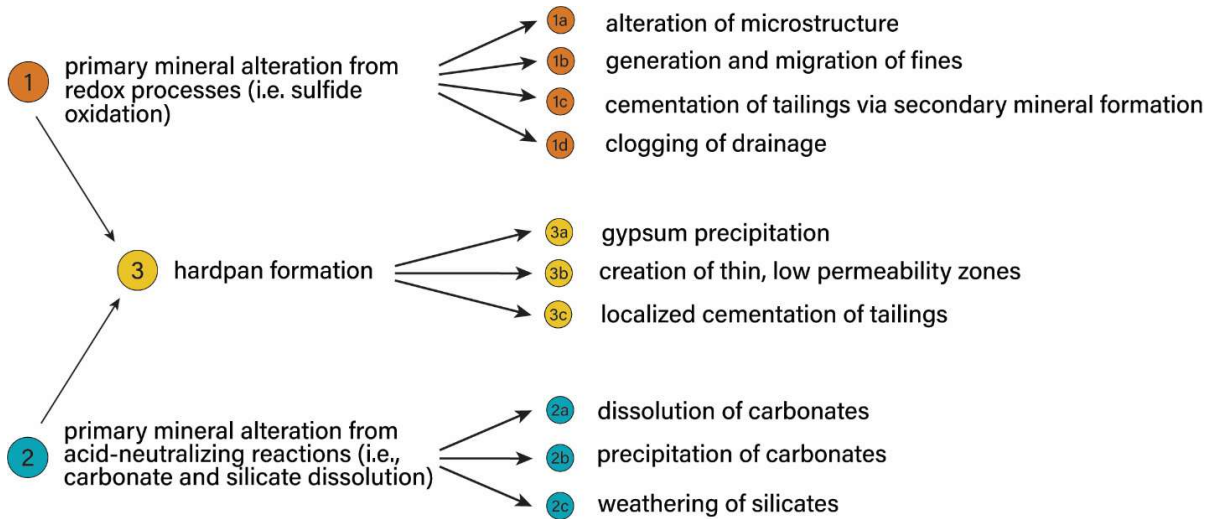


Figure 3: Process map breaking down major geochemical processes occurring within a tailings storage facility.

2.3.1. Primary Mineral Alteration from Redox Processes

Primary mineral alteration from redox reactions includes the oxidation of primary sulfides (i.e., pyrite, pyrrhotite, etc.) to secondary metal-oxides and oxyhydroxides (Durocher, 2023). Sulfide oxidation occurs via physical, chemical, and biological weathering. To encapsulate all these processes, the following four categories were identified as the major weathering processes of primary minerals occurring via redox reactions relevant to geotechnical stability of tailings: (1a) alteration of microstructure; (1b) generation and migration of fines; (1c) cementation of tailings; and (1d) clogging of drainage. Many studies, for example, focus on the decrease in average particle size due to weathering and, as such, the “generation and migration of fines” summarizes all these

works, the relevant geochemical processes involved with breakdown of particles, and allows for discussion on the further implications to geotechnical stability.

2.3.1.a. Alteration of Microstructure

Figure 4 shows the breakdown of primary minerals (pyrite, pyrrhotite) from angular, rough, granular sized minerals to smooth, curved amorphous secondary minerals (ferric hydroxide, $\text{Fe}(\text{OH})_3$). The alteration of particle microstructure results from various physical, chemical, and biological weathering processes. A case study by Wang et al. (2023) examined changes to the particle microstructure and interlocking of weathered lead (Pb) and zinc (Zn) tailings and determined that weathering resulted in the breakdown of rough, angular primary minerals into smooth, smaller fragments that exhibited less interlocking. An important note is that this is not universal for all tailings weathering byproducts or secondary mineral precipitates. For example, jarosite is a crystalline metal-hydroxy-sulfate and typically forms compact, intergrown granular masses (Bryant, 2003; Ridley, 2023). However, changes to the microstructure (i.e., surface texture) may be useful in explaining a decrease in shear strength following formation of amorphous iron oxides and/or phyllosilicate minerals.

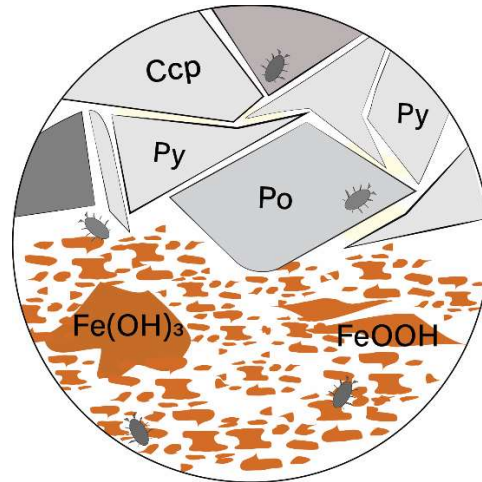


Figure 4: Conceptual schematic of the alteration of rough, crystalline primary minerals such as pyrite (Py) and pyrrhotite (Po) to smooth, amorphous secondary minerals (e.g., ferric hydroxide, $\text{Fe}(\text{OH})_3$).

Wang et al. (2023) evaluated the friction angle and cohesion of Pb-Zn tailings under different degrees of oxidation and analyzed the microstructure with Scanning Electron Microscope (SEM) imagery. They observed a decrease in internal friction angle with an increase in the degree of oxidation due to weathered minerals having less particle roughness and interlocking than unweathered surfaces, as well as a decrease in cohesion force due to dissolution of carbonate cements. This is consistent with other geotechnical studies which observed a reduction in shear strength of fine-grained soils due to weathering reactions (Filipowicz and Borys, 2005; Seedsman and Emerson, 1985) or upon interaction with acidic pore fluids (Gratchev and Towhata, 2013).

2.3.1.b. Generation & Migration of Fines

Figure 5 shows finer particles as more easily transported than coarse particles, migrating downwards, clogging pores, and inhibiting the transport of water and/or oxygen (Blowes et al., 1998). As primary minerals break down, the generation and migration of fines decreases

the average particle size and widens the particle size distribution (Blowes et al., 1998; Carelson, 2013; Elghali et al., 2021; Forsberg and Ledin, 2001; Lin, 1997). Conversely, over time, iron oxides and clay minerals can form aggregate particles, increasing the average particle size again (Stucki et al., 1987). An overall reduction in particle size also increases water retention, as fine-grained tailings exhibit higher suction stresses capable of retaining water due to capillary forces. In addition, fine-grained materials typically have low permeabilities and are slow to dissipate excess pore water pressures during loading, resulting in higher water contents, less self-weight consolidation, and a tendency to shear undrained. Smaller particles are also more susceptible to weathering due to their increased surface area (Dultz, 2002; Morkeh and McLemore, 2012). These negative impacts of fines are why, for most design purposes, the sand fraction used in tailings dam construction is required to have a fines content $< 20\%$ (Zhang et al., 2020). However, a sand fraction that begins with a fines content $< 20\%$ may not remain so.

Conversely, well-graded soils are also more likely to form denser packings, as smaller particles fill the voids between larger particles. A denser packing is advantageous in that dense materials tend to generate negative pore water pressures under loading, increasing their resistance to shear. Dense materials also have more tortuous flow paths which would limit O_2 ingress and further sulfide oxidation (Duncan et al., 2014; Devasahayam, 2006).

Secondary mineral precipitates also have a higher specific surface area (SSA) than primary minerals, resulting in an increased affinity for ions and water (Lin, 1997; Forsberg and Ledin, 2001; Elghali et al., 2021). Due to the surface charge of most iron oxides and clays, water is electrostatically retained, lowering permeability, compressibility, and water release. This hinders drawdown and self-weight consolidation of the material. Following the

same principles, Stucki et al. (1987) discuss the aggregation of iron oxides due to attraction between the positive variable surface charge of iron oxides and the permanent negative surface charge of clay minerals, so while the surface charge of secondary iron oxides may lead to a higher affinity for water, likewise the aggregation of iron oxides can result in less inter-particle void space and higher internal friction angles (Ng et al., 2019).

An important distinction to make at this point is between fines generation, aggregation, and cementation (i.e., ferricrete, calcrete, etc.). Fines can simply be generated and advected without any significant flocculation, like sediment moving down a river. Cementation, however, occurs at high iron contents and when iron oxides grow in pores, expanding until there is a high surface contact between the iron oxides and growth media (Stucki et al., 1987). Aggregation is achievable at lower iron contents and occurs due to electrostatic bonding between mineral surfaces (Stucki et al., 1987). Lastly, hardpan formation consists of cementitious materials and will be discussed more in Section 2.3.3. Fines generation is generally going to result in stability concerns related to water management failures, whereas cementation and aggregation may result in brittle behavior from bond formation within loose tailings and/or a reinforced soil skeleton with more particle interlocking.

2.3.1.c. Cementation of Tailings

As iron oxides form and fill intergranular pores, they encapsulate tailings particles and form a light cement around them. Figure 5 shows light cementation occurring between tailings particle contacts. Cementation is different from “hardpans,” which are thick, impenetrable layers that form from a combination of secondary minerals such as goethite and gypsum (Lin et al., 1997).

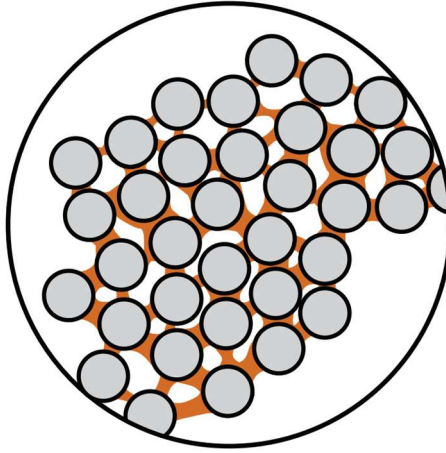


Figure 5: Light cementitious bridges of secondary Fe-minerals forming between particles.

Sulfide oxidation in the active oxic zone releases ferrous iron (Fe^{2+}) which remains dissolved due to high solubility in acidic pore waters. As Fe^{2+} rich water migrates into less acidic zones, Fe^{2+} is oxidized to ferric iron (Fe^{3+}) which begins to precipitate under neutral conditions. Depending on the source zone of these sulfidic “hotspots” and/or the transport of the Fe-rich pore water, iron oxide formation can occur anywhere where an increase in pH and/or redox is observed (transition zone, embankment materials, foundation, etc.).

As iron oxides form and fill intergranular pores, they form bridges between particles like capillary bridges (Carelson, 2013). Lin et al., (1997) identified goethite as the primary cementitious material surrounding silicate particles and reducing permeability in their case study. Particularly of concern is when cementation occurs in the tailings embankment structure zone and creates a stiff, brittle material that has high peak strength and low residual strength, as seen in the Brumadinho dam failure (Robertson et al., 2019).

Conversely, a study by Power et al. observed an increase in the unconfined compressive strength (UCS) of ultramafic tailings via brucite ($\text{Mg}(\text{OH})_2$) precipitation within tailings

particles (2021). Likewise, Forsberg and Liden (2001) reported that cementation of weathered vs. unaltered tailings increased the penetration resistance of laboratory and field samples when comparing material suitable for revegetation. Overall, the mineralogy and long-term geochemical stability of the cementitious mineral is important to determining if cementation is a reliable reinforcement option into perpetuity and further analysis of the brittle behavior of cemented tailings should be conducted.

Cementitious soils also have a low compressibility due to their rigid soil skeleton. Lateritic soils containing goethite were observed to have a compressibility 18% and 36% lower than soils containing less Fe- and Al-oxides (Ng et al., 2019). The lateritic soils were less compressible due to a decrease in inter-particle void space upon aggregate formation, the latter of which contributed to a higher internal friction angle due to more particle interlocking (Ng et al., 2019). Overall, distinguishing between secondary Fe-bearing minerals and type of formation (fines, aggregates, cements) is important due to the wide range of strength properties, as described insofar. For example, goethite has a hardness of 5-5.5 on the Mohs hardness scale which contributes to a rigid soil skeleton, whereas jarosite has a hardness of 2.5-3.5 (Mukherjee, S., 2012; Ng et al., 2019).

2.3.1.d. Clogging of Drainage

As Fe^{2+} rich water migrates through the drainage layer, a collection system transports the dissolved iron from a reduced (anoxic) environment to an oxidized (oxic) environment. Upon contact with oxygen in the atmosphere, Fe^{2+} oxidizes to Fe^{3+} . As this water transports further away from the acidic source zone and neutralizes, Fe^{3+} precipitates begin to form (Nordstrom et al., 2015). In addition, calcite precipitation can occur due to a high partial pressure of dissolved CO_2 in the TSF pore water because of microbial activity, gypsum,

and iron oxy-hydroxide formation, which must equilibrate with atmospheric CO_2 through exsolving of carbonate. Lastly, dissolved silica ($\text{SiO}_{2(\text{aq})}$) from primary silicate mineral dissolution may precipitate as opal and/or chalcedony in drainage pipes (Ridley, 2023). Figure 6 shows the results of these precipitation reactions occurring, effectively clogging the drainage system over time.

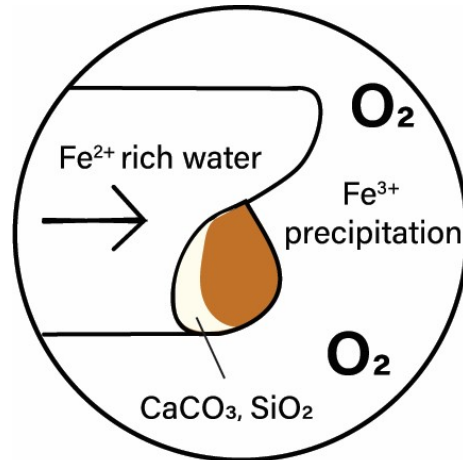


Figure 6: Clogging of drainpipes due to secondary mineral precipitation. Fe^{2+} , aqueous ferrous iron, shown precipitating as Fe^{3+} under oxidizing conditions. Calcite (CaCO_3) precipitation under atmospheric partial pressure of CO_2 and amorphous silica mineral formation (SiO_2).

Wu et al. (2007, 2008) studied the kinetics and influence of pH on pipe clogging and determined that precipitation rates increased significantly at $\text{pH} > 7$ and within 23 days of their study the pipes were completely clogged. Pipe clogging inhibits drainage, which causes a rise in the phreatic surface and pore water pressure. High pore-water pressures result in low effective stress and reduced self-weight consolidation. Loose, contractive materials with high water contents are at risk for liquefaction if the material were to shear undrained.

Bioclogging, or the inhibition of drainage due to growth of biological life, can also inhibit drainage. Smaller particles have a high specific surface area to support biotic life; therefore,

the migration of sediments from weathering can promote bioclogging and fouling (Rowe et al., 2000).

2.3.2. Primary Mineral Alteration from Acid-Neutralizing Reactions

Acid-neutralizing reactions involve the dissolution of soluble minerals such as carbonates, silicates, and Al- and Fe-(oxy) hydroxides (Durocher, 2022). As these minerals dissolve, their ions remain in solution and have the potential to reprecipitate under various environmental conditions. As such, the following categories summarize the geochemical evolution of tailings via acid-neutralizing reactions as relevant to geotechnical stability: (a) dissolution of soluble mineral phases; (b) precipitation of soluble mineral phases; and (c) weathering of silicates to clays.

2.3.2.a. Dissolution of Carbonates

Dissolution of carbonates (and/or other soluble minerals) is shown schematically in Figure 7. Carbonates (minerals containing CO_3^{2-}) are common in tailings deposits and are well-studied due to their ability to buffer pH and limit ARD. Calcite (CaCO_3) is one of the most common carbonate minerals and dissolves readily in acidic water. Other types of carbonates often exist in tailings deposits such as siderite (FeCO_3), dolomite ($\text{CaMg}(\text{CO}_3)_2$), and/or ankerite ($\text{Ca}(\text{Fe},\text{Mg})(\text{CO}_3)_2$) but may be less reactive (Mitchell and Soga, 2005).

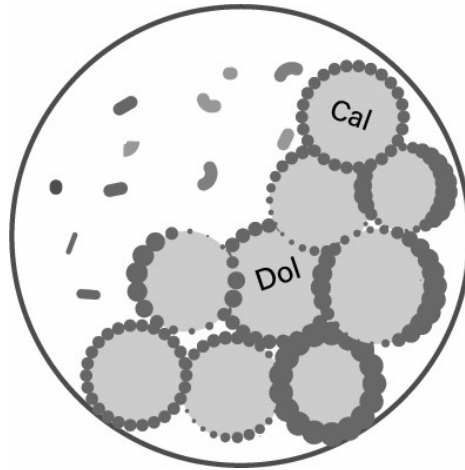


Figure 7: Dissolution of soluble mineral phase (e.g., calcite, Cal and dolomite, Dol) leading to dissolved calcium and carbonate ions in solution.

The dissolution of soluble minerals can result in mass loss, internal erosion, piping, and increased hydraulic conductivity via preferential flow pathways. Mass loss may yield increased tailings compressibility (higher void ratio) and a tendency towards more brittle flow-type shear behavior (contractive). However, dissolution will also reduce tailings unit weight.

2.3.2.b. Precipitation of Carbonates

Reprecipitation of dissolved minerals is shown schematically in Figure 8. Migration of $\text{CO}_{2(g)}$ from precipitation reactions and microbial activity can promote precipitation of carbonate minerals between particle contacts at the surface. At greater depths in the TSF (or rock pile), higher partial pressures of CO_2 and lower partial pressures of O_2 are found as oxygen is depleted near the surface (Shaw et al., 2002). As the dissolved mineral phase (Ca^{2+} ions and $\text{CO}_{2(g)}$) migrate to the surface of a TSF, the high partial pressure of $\text{CO}_{2(g)}$ in solution must equilibrate with atmospheric CO_2 by precipitating carbonates.

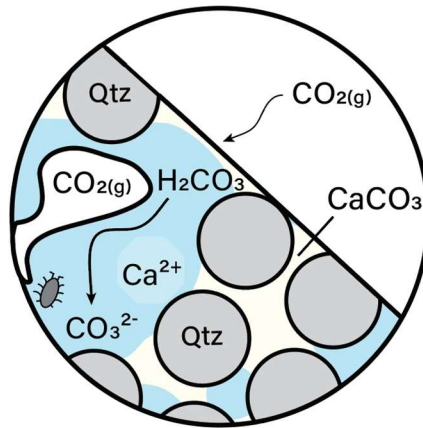


Figure 8: Precipitation of soluble mineral phase (e.g., calcite, CaCO_3) between tailings particles (quartz, Qtz). Reprecipitation occurs due to supersaturation of calcium (Ca^{2+}) and carbonate (CO_3^{2-}) and high partial pressure of CO_2 in the tailings reaching atmospheric equilibrium.

Precipitation of soluble mineral phases can result in reduced porosity which may hinder drainage and consolidation. Precipitation of carbonate minerals can also form cementitious material with low compressibility and higher resistance to shear (Power et al., 2021; Wang et al., 2023).

2.3.2.c. Weathering of Silicates to Clays

Silicate minerals (e.g., feldspar, plagioclase, micas, olivine, etc.) are primary minerals that undergo physical, chemical, and biological weathering over time to transform into more stable phyllosilicates (clays). For example, feldspar weathers to kaolinite via hydrolysis (Mitchell and Soga, 2005). Whereas feldspar is a crystalline primary mineral, kaolinite may produce weak clay layer(s) with significantly lower shear strength than the source primary mineral. Figure 9 shows the breakdown of silicate minerals to phyllosilicate clay layers in embankment materials due to interaction with water, separated here by hydrogen (H^+) and hydroxide (OH^-) ions.

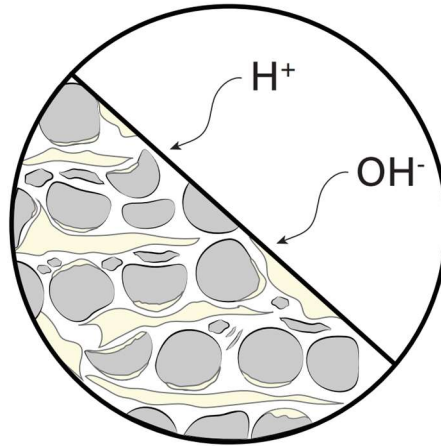


Figure 9: The breakdown of primary silicate minerals in embankment to secondary phyllosilicate clay layers via hydrolysis (interaction with H^+ and OH^-). Interface between embankment materials and atmosphere is delineated by the black line.

Often, the slow rate of hydrolysis has been cause for disregard of the breakdown of silicate minerals within mine wastes (as seen in the Questa Rock Pile Stability Reports); however, the smaller particle size of tailings minerals compared to waste rock can significantly enhance the rate of hydrolysis (Dultz, 2002; Morkeh and McLemore, 2012). An example of silicate dissolution occurring with a TSF can be seen in Lin et al., (1997) in which primary silicates (chlorite and biotite) transformed to vermiculite, illite, and smectite in the active oxidation layer of a TSF due to high levels of acidity from sulfide oxidation and availability of oxygen due to near-surface conditions.

The formation of clays can also fill void spaces, reduce permeability, and reduce self-weight consolidation. A paired geotechnical and geochemical report on the San Manuel TSF observed ductile behavior within the weathered tailings, giving rise to concern for cementation occurring via calcite and/or iron -oxide and -oxyhydroxide precipitates; however, the geochemical analysis revealed the presence of phyllosilicates (illite, kaolinite,

and montmorillonite) (Casey et al., 2022; Kotzer et al., 2022). Pore clogging via the mica-silica mixed phase was observed via computerized tomography (CT) and was hypothesized to potentially contribute to brittle behavior due to aggregate formation (i.e., cementation) from the electrostatic bond between clay particles.

Phyllosilicate clay layers can also exchange cations (Ca^{2+} , Na^+ , K^+) and, based on the availability of nutrients, the pore water chemistry of seepage, and the cation exchange capacity of clays, the double diffuse layer (DDL) can shrink or swell, which further alters permeability and water content (McBride, 1994). Shrink/swell behavior can also result in differential settlement and consolidation (Mitchell and Soga, 2005).

Lastly, acidic seepage can alter the strength properties of clay minerals in the foundation. Gratchev and Towhata (2013) studied the effects of pH on montmorillonite and kaolinite and observed a reduction in shear strength for both materials. Spagnoli et al. (2012), however, observed an increase in internal friction angle of kaolinite at high and low pH values due to flocculation of Al^{3+} and changes in soil fabric. Therefore, understanding the mineralogy of a given site and the anticipated changes to pore fluid chemistry can provide insight on the long-term geotechnical properties of weathered materials.

2.3.3. *Hardpan Formation*

A conceptual schematic of hardpan formation is shown in Figure 11. Hardpans are aerially extensive but vertically thin cemented layers that can form within a TSF. They consist of secondary mineral precipitates such as lath or fibrous crystals of gypsum ($\text{CaSO}_4 \cdot 2\text{H}_2\text{O}$) interbedded with iron oxy-hydroxides (e.g., goethite ($\alpha\text{-FeOOH}$)) and iron sulfates (e.g., jarosite ($\text{KFe}_3(\text{SO}_4)_2(\text{OH})_6$)) (Lin, 1997; Lui et al., 2019; McGregor and

Blowes, 2002). Hardpans are commonly formed in zones which exhibit a contrast in pH, redox, or chemical composition (Blowes et al., 1991, 1998; Elghali et al., 2019; Lottermoser and Ashley, 2006; McGregor and Blowes, 2002; Pérez-López et al., 2007). Hardpans can also form following the placement of a cover as the system transitions from oxic to anoxic (Alakangas and Öhlander, 2006) or at the interface of the oxic and transition zone. In general, tailings with higher sulfide content and/or higher pyrrhotite content form cemented layers more readily due to the fine-grained nature of pyrrhotite, resulting in a higher rate of reaction (Agnew and Taylor 2000; Ahmed, 1995). Generally, hardpans are orange if formed at the surface or green-grey if formed at depth and have low permeabilities and high resistance to shear.

2.3.3.a. Gypsum Formation

Gypsum formation is a combined process involving both sulfide oxidation and soluble mineral dissolution, and, as mentioned above, often forms the cement of hardpans. The oxidation of sulfides provides the sulfate ion (SO_4^{2-}), whereas carbonate dissolution provides the calcium ion (Ca^{2+}). Gypsum ($\text{CaSO}_4 \cdot 2\text{H}_2\text{O}$) is one of the most common weathering products in TSFs and plays an integral role in hardpan formation (Alakangas and Öhlander, 2006; Blowes et al., 1998; Elghali et al., 2019; Lin, 1997; Lui et al., 2018; McGregor and Blowes, 2002). Gypsum is also notorious for inducing heave due to the relatively lower density of gypsum ($G_s = 2.3$) compared to the original reactants, pyrite ($G_s = 4.8\text{-}5.1$) and calcite ($G_s = 2.7$) (Bryant, 2003; Hawkins and Pinches, 1997). As a sulfate crystal, gypsum also has the tendency to form along discontinuities due to lower confining stresses in these regions, such as along discontinuities in pyritic shale (Bryant, 2003; Mitchell and Soga, 2005). Gypsum has a relatively high solubility ($K_{sp} = 4.59$) and is

more likely to form in unsaturated zones with neutral pH values, such as in the upper regions of a TSF and/or along the embankment (Bryant, 2003). Figure 10 shows gypsum formation occurring along a discontinuity in the foundation and resulting in heave ($+\Delta V$).

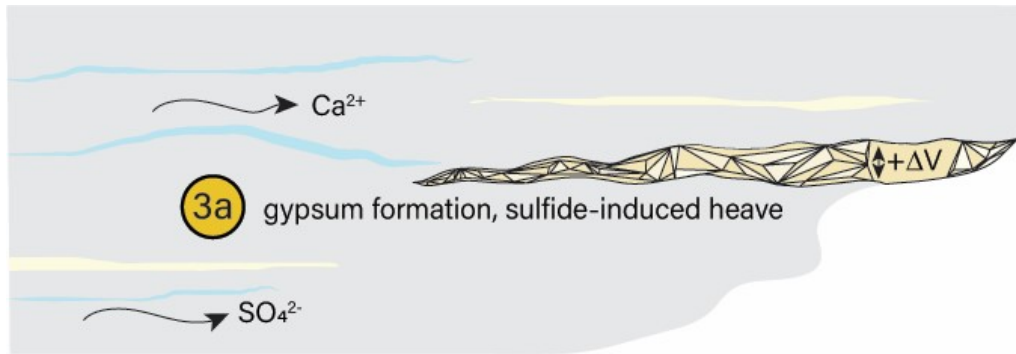


Figure 10: Schematic of sulfide-induced heave occurring via gypsum formation from the reaction of calcium ions (Ca^{2+}) and sulfate ions (SO_4^{2-}) along discontinuity in bedrock.

2.3.3.b. *Creation of Low Permeability Zones*

The creation of low permeability zones can mislead stability analysis if perched water tables go undetected. Hardpans have a high bulk density and low porosity that limits the movement of water and gas in and/or out of the system (McGregor and Blowes, 2002). As such, hardpans have been extensively studied for their potential as effective, low-cost cover systems due to their ability to limit infiltration, increase runoff, and limit sulfide oxidation via reduced gas transport (Liu et al., 2021).

However, hardpans can simultaneously prevent water infiltration and entrap water by preventing evaporation from a TSF (Figure 11). Hardpans have been demonstrated to slow the rate of gas transport due to their low permeability. Blowes et al. (1991) calculated an oxygen diffusion coefficient 100x slower for the hardpan layer vs. uncemented tailings. They

also detected a 45% increase in pore gas CO₂ concentration below the hardpan due to carbonate dissolution and degassing rising from deeper levels within the TSF yet remaining trapped.

In addition, perched water tables may form above the hardpan layers, creating zones of low shear strength. Porewater within the perched water table will eventually become supersaturated in heavy metals and form metal-sulphate precipitates (e.g., PbSO₄, ZnSO₄). Perched water tables were detected in the Questa rock piles and led to inaccurate reports of degree of saturation and infiltration, compromising the validity of stability analysis (Bryant, 2003). Figure 11 shows hardpan formation at the interface between the oxic zone (orange) and transition zone (yellow), preventing vertical flow of oxygen and water.

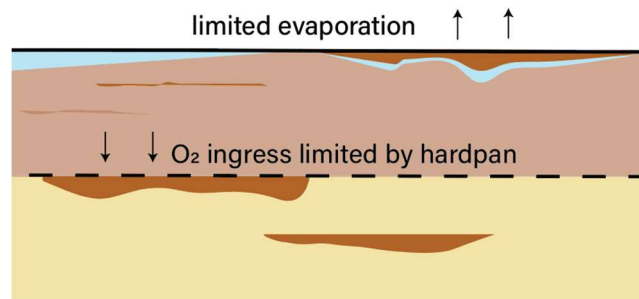


Figure 11: Hardpan formation at interface between oxidized zone (orange) and transition zone (yellow). Hardpans limits oxygen ingress (sulfide oxidation) and evaporation (desiccation).

2.3.3.c. Localized Cementation of Tailings

Hardpans, or cemented layers, form thick, impenetrable layers that are resistant to shear and erosion and have been studied for the ability act as effective cover systems (Ahn et al., 2011; Alakangas and Öhlander, 2006; Blowes et al., 1991; Elghali et al., 2021; Lin et al., 1997, Lui et al., 2019; McGregor & Blowes, 2002). A study by Ahn et al. (2011), studied the

strength properties of engineered hardpan covers and found hardpans augmented by waterglass (forms a calcium silicate binder) to exhibit compressive strength properties sufficient to be considered pavement by ASTM definitions.

However, hardpans are also subject to environmental conditions and will undergo alteration over time. For example, hardpans that have coprecipitated arsenic as scorodite and amorphous hydrous ferric arsenate (HFA) will later dissolve the cement if the acid-generating sulfides are depleted and the pH approaches circumneutral values (DeSisto et al., 2011). Likewise, cementing minerals may be dissolved if the system transforms from oxidized to reduced during cover placement (Alakangas and Öhlander, 2006). Therefore, the geochemical alteration of the hardpan over time and performance under different environmental conditions must be considered if eco-engineering a hardpan to reinforce tailings and/or improve effluent water quality.

2.4. Influence on Potential Failure Modes

Failure is defined by Davies et al. (2002) as “...an unacceptable difference between expected and observed performance”. Physical, chemical, and biological weathering of tailings will alter tailings physical properties over time, yielding changed characteristics that may result in an unacceptable difference from design conditions. Understanding, and when necessary, accounting for changes in material properties due to weathering reactions is an important aspect of tailings management that has not received sufficient attention. There is still much to be understood in terms of geochemical weathering and the resulting impact on long-term geotechnical stability.

In this section I draw connections between the geochemical processes that impact geotechnical parameters described in the preceding section and potential TSF failure

modes. The focus here is on dam stability failure modes, rather than environmental or governance failures. When possible, I link failures that have been analyzed for the influence of geochemical weathering reactions on geotechnical properties.

Potential failure modes are grouped as: (1) flow-type stability failure; (2) water management related failure; (3) piping and internal erosion failure; and (4) foundational failure. This is designed to coincide with high-level dam failure modes as defined by the International Commission on Large Dams (ICOLD); however, ‘water management’ has been chosen in lieu of alternatives (such as slope instability, overtopping, etc.) to encapsulate the wide range of geochemical processes that have an impact on water related issues, and ‘flow-type stability behavior’ has been chosen due to the lack of information on the liquefaction behavior of cemented soils (ICOLD, 2001).

2.4.1. Flow-type Stability Failure Mode

Figure 12 illustrates the increased possibility of flow-type stability failures due to tailings weathering. An increased tendency towards brittle behavior may be caused by precipitation of minerals at grain contact yielding a more stiff and contractive tailings fabric. For example, goethite has a high hardness value of 5-5.5 and has been observed to develop rigid soil skeletons that resist compression (Mukherjee, S., 2012; Ng et al., 2019). In addition, the generation of secondary iron oxides and oxyhydroxides can hinder drainage and result in a buildup of pore water pressure behind the dam face. If undrained shearing is initiated, the material may undergo flow liquefaction due to an increased tendency to shear undrained (low permeability of weathered tailings) and contractive nature (limited consolidation of cemented tailings) (Davies et al., 2002).

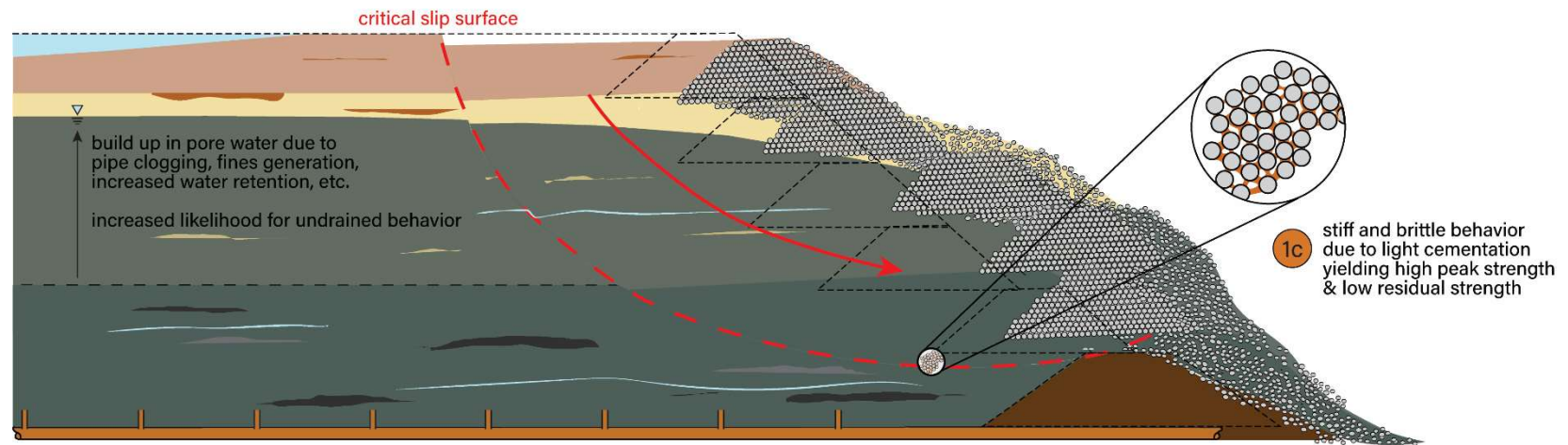


Figure 12: Potential flow-type stability failure mode due to cementation of embankment materials creating a brittle, stiff, and contractive material. Advanced weathering causes a buildup of pore water pressure and the development of a critical slip surface.

The Brumadinho TSF failure in Brazil in 2019 brought significant loss of life and environmental damage and has since proven to be a turning point in tailings management. One of the identified potential causes of failure was the high iron content within the tailings embankment materials (> 50%) that, even upon remolding, demonstrated brittle behavior and showed light cementation between tailings sand particles (Robertson et al., 2019). Light cementation potentially hindered self-weight consolidation, yielding a higher void ratio at an equivalent effective stress. Of note, geochemical processes that lead to precipitation in tailings pore space are not unique to iron-rich tailings. Instead, cementation is a result of aqueous Fe^{2+} oxidizing to Fe^{3+} upon interaction with the atmosphere, forming ferric iron oxides and oxyhydroxides bridges between tailings particles and/or the precipitation of carbonate minerals in tailings pore space as dissolved ions and high partial pressures of CO_2 equilibrate with the atmosphere.

2.4.2. Water Management Failure Mode

A conceptual schematic of different potential water management failure modes is provided in Figure 13. Slow drainage, increased pond size, and an elevated water table are all common water management concerns when discussing tailings dam stability. The result of weathering reactions, (1b) generation and migration of fines; (1c) cementation; (1d), drainpipe clogging; (2b) soluble mineral precipitation; (2c) weathering of silicates to clays; and (3) hardpan formation, can all increase the possibility that one or many of these water management concerns requires mitigation over the lifetime of a TSF to minimize potential failure modes.

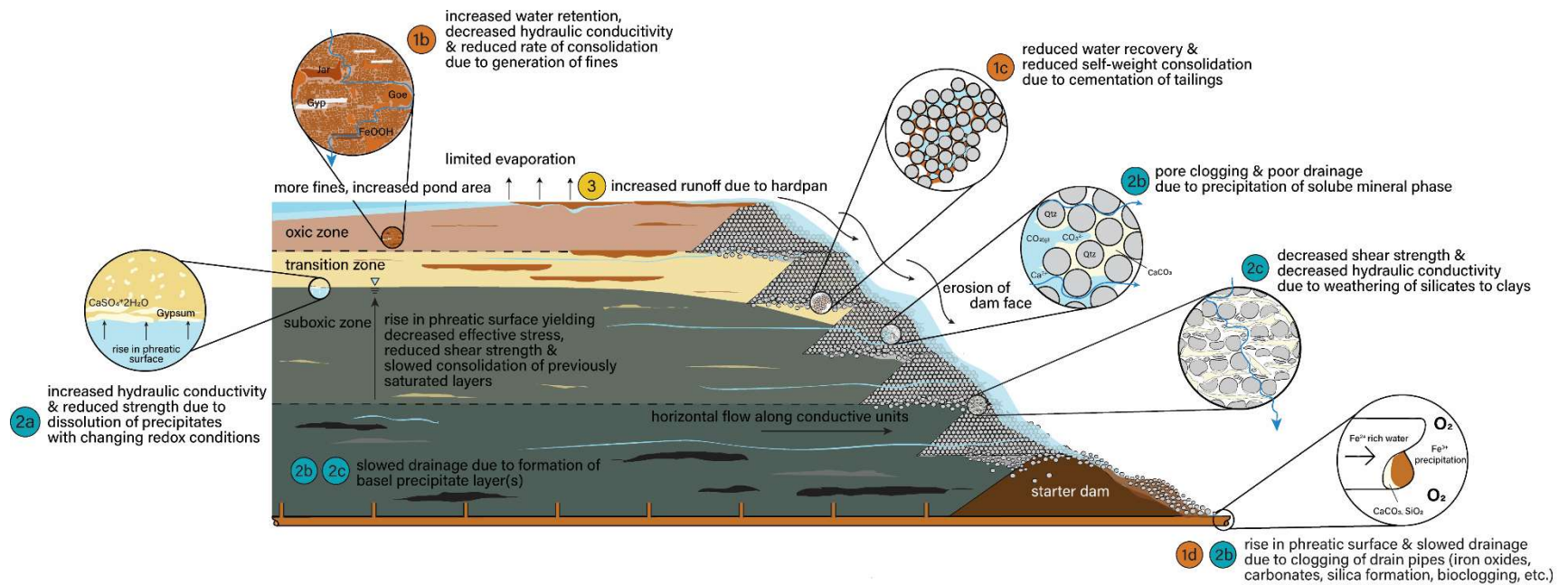


Figure 13: Schematic of water management failure due to a series of weathering reactions. Failure includes hindered drainage, erosion due to overtopping, slope instability, increased liquefaction potential, and more.

Weathering, as explained in the previous section, may reduce average particle size and hydraulic conductivity of oxidized tailings, slowing the rate and magnitude of self-weight consolidation and increasing degree of saturation. Poor drainage of oxidized materials at the tailings impoundment surface can increase the pond area and lead to overtopping if the pond were to encroach upon the embankment. Slowed consolidation and high water contents can also result in a loose, contractive fabric with an increased likelihood of failing undrained (no change in volume during shear, $\Delta V = 0$) due to the low hydraulic conductivity of the material. In worst case scenarios, loosely deposited tailings that fail undrained can experience a rapid increase in positive pore water pressure, a subsequent decrease in shear strength, and potential flow liquefaction (Davies et al., 2002). Liquefaction is the most catastrophic type of tailings dam failure due to a near-instantaneous nature and wide-spread impact, which can be both fatal to human life and deleterious to the downstream environment.

The dissolution of carbonates within the tailings matrix, foundation, and/or embankment construction materials can result in zones of increased hydraulic conductivity, mass loss, and preferential flow paths (i.e., piping and/or internal erosion). In addition, calcite precipitation can clog pores, hinder drainage, and create zones with a hardened soil structure which resist consolidation and compression. Other water management concerns include clogging due to precipitation of iron oxides, silica formation, and/or calcite precipitation, which can hinder drainage and lead to a raised water table, increasing the likelihood for an undrained failure and a reduction in shear strength. Lastly, perched water tables have been observed in the Questa rock piles due to the generation of fines and/or

clays which inhibit drainage and encourage precipitation of oversaturated minerals (URS Corporation, 2001).

2.4.3. Internal Erosion and Piping Failure Mode

Figure 14 shows a conceptual schematic of how geochemical processes may yield internal erosion and piping failure modes. Internal erosion is defined as the moment in which the, “hydraulic gradient and velocity is sufficient to overcome the geometric fabric and stability of the soil structure” causing the movement and migration of soil particles, whereas piping “describes the behavior of the soil structure when internal erosion develops a continuous open seepage path” (Clarkson and Williams, 2021). The dissolution of carbonates and other soluble minerals (2a) in the embankment structural zone can create conduits for flow, increasing risks of internal erosion and piping (Clarkson and Williams, 2021; Fell et al., 2015). Soluble mineral dissolution will be accelerated by acidic pore water and can even reprecipitate dissolved minerals in less acidic and/or oxidized zones. If the water table is above the piping failure, perhaps due to other weathering reactions, the transportation of water and sediment can erode the dam face until failure occurs.

Properties indicative of internal erosion and piping failures are plasticity (i.e., interparticle bond strength), gradation and particle size, density, and erodibility (Clarkson and Williams, 2021; USBR, 2015). Therefore, cementation via iron oxidation and/or carbonate precipitation is likely to reduce susceptibility to erosion due to the generation of higher inter-particle bond strength; however, secondary minerals are less dense than parent materials, decreasing the amount of energy required for transportation, and the dissolution of carbonates results in a less dense, well-graded material more susceptible to erosion (Clarkson and Williams, 2021).

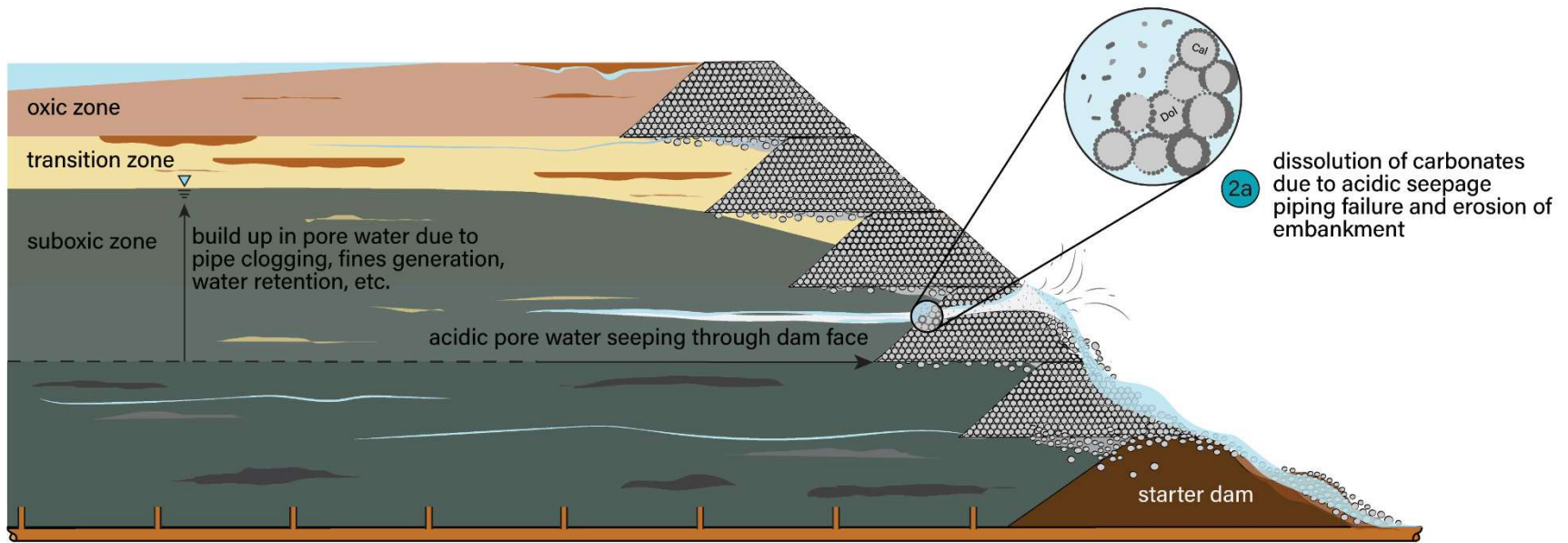


Figure 14: Schematic demonstrating internal erosion and piping failure mode accentuated by alteration of the soluble mineral phase and the buildup of pore water due to various geochemical processes.

2.4.4. Foundational Failure Mode

The foundation of a TSF is critical to stability and Figure 15 provides a conceptual schematic for potential failure modes tied to TSF foundations. Clarkson and Williams (2021) highlight isolated karst deposits, deeply weathered rock, cohesionless soils, and carbonate dissolution as potential foundation concerns. These concerns are well recognized, and any new facility will undergo an extensive site investigation to get an in-depth analysis of the foundation conditions; however, the foundation of any TSF is subject to seepage water quality and groundwater flow and, as such, may undergo alterations due to weathering processes. For example, acidic seepage generated from sulfide oxidation can dissolve karst deposits over time and form large cavities and/or create conduits for groundwater flow that can be both structurally compromising and environmentally damaging.

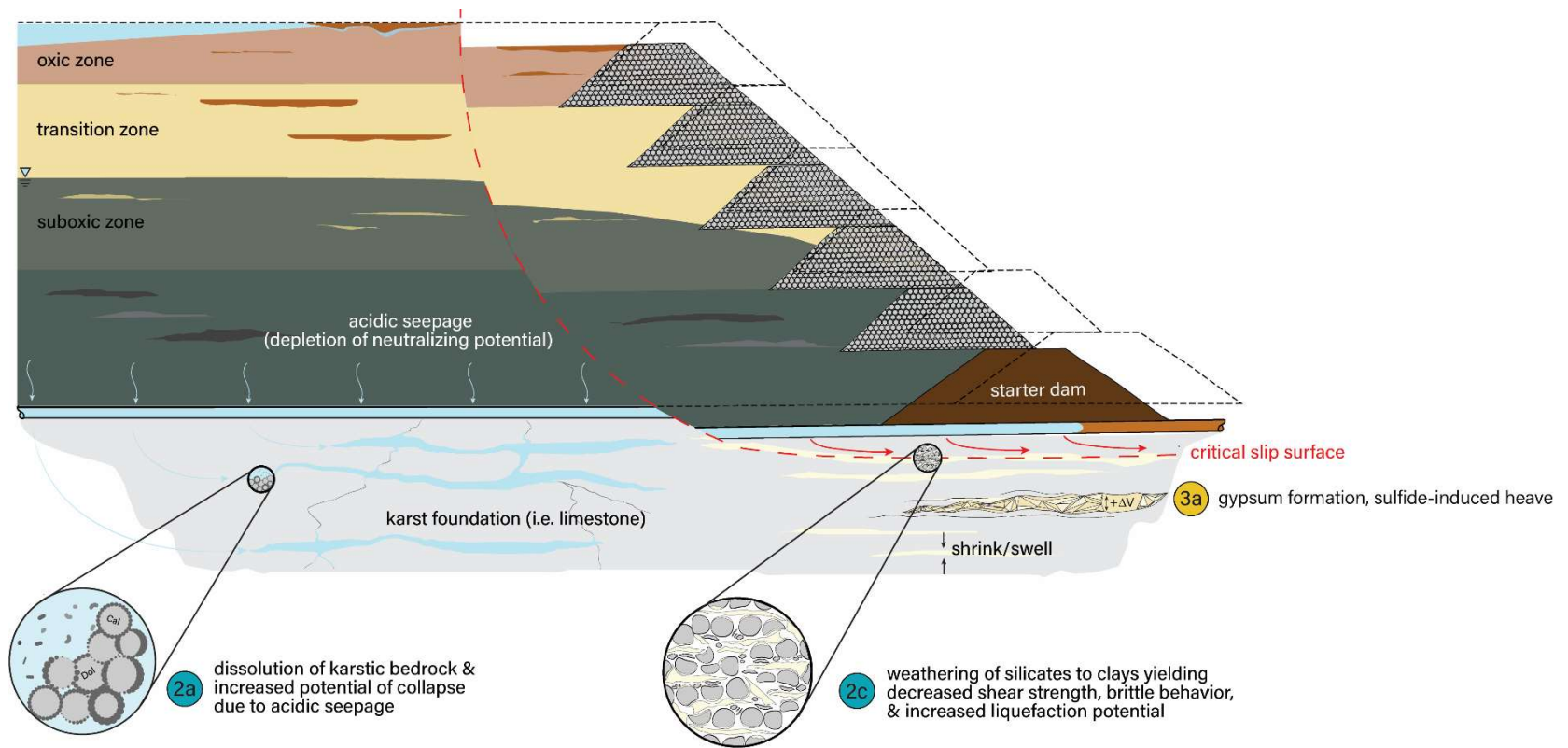


Figure 15: Schematic demonstrating potential foundational failure modes via karstic bedrock dissolution, clay formation, and sulfate-induced heave via gypsum formation along discontinuities. Formation of critical slip surface under embankment shown in red.

Low permeability and high permeability foundations exhibit different groundwater flow patterns and have different failure potentials (Clarkson and Williams, 2021). Low permeability foundations can be formed due to weathering of parent rock (clay formation) and soluble mineral precipitation, whereas high permeability formations can be formed due to mineral dissolution (i.e., karst deposit dissolution). Low permeability foundations often consist of clays and/or weathered material that have a low shear strength and can fail undrained due to the slowed drainage that retains excess pore water pressures upon loading (Clarkson and Williams, 2021). High permeability foundations can transmit flow capable of eroding material at the base of the embankment (Clarkson and Williams, 2021). In addition, foundations are capable of transporting groundwater laden with suspended/colloidal minerals and, if the environmental conditions are favorable, soluble mineral precipitation can clog pores and lower the effective hydraulic conductivity. Ultimately, the phreatic surface within the TSF will be influenced by the geochemical processes that control the permeability of the foundation. Simultaneously, the foundation permeability will be influenced by seepage water quality.

Foundational failures induced by pyritic rock and soil are outlined and synthesized by Bryant (2005). Example case studies include the damage of over 1000 homes in Japan due to microbially induced sulfidic heave of pyritic mudstone, resulting in maximum deformation of 48 cm (Yamanaka et al., 2002). The deformation was largely due to acid generation via sulfate-reducing, sulfide-oxidizing, and iron-oxidizing bacteria, which then led to volume increase via gypsum and jarosite formation and an increase in voids due to carbon dioxide gas generation (Bryant, 2005; Yamanaka et al., 2002).

Another case study, Carsington Dam, involved the death of four workers due to build up of excess carbon dioxide concentrations and clogging of drainage pipes. The $\text{CO}_{2(g)}$ was generated due to sulfide oxidation of pyritic mudstone, which led to acid generation capable of dissolving the carboniferous limestone drainage blankets. These then clogged with gypsum and iron oxide precipitates, entrapping the carbon dioxide gas (Cripps et al., 1993).

Lastly, the presence of brittle clays and/or weathered volcanic rock within the foundation may lead to global failure, as seen in the Aznacóllar and Cadia failure, respectively (Gens and Alonso, 2006; Gleeson et al., 2020).

2.5. Monitoring Potential Failure Modes

The previous tailings dam failures are not mentioned to raise alarm or insist that every facility needs to rapidly develop a geochemical monitoring plan; however, recognizing and expounding upon the influence of geochemical processes in previous failures is essential to preventing the same mistakes from happening again. Currently, many unknowns remain as to how all these geochemical processes interplay with one another – if they are advantageous or deleterious, if they are occurring at a rate significant enough to be addressed in the present moment, etc. Nature is complex, and isolating any one of these geochemical processes in a laboratory setting is unlikely to provide useful information on a large enough scale. The following sections outline approaches to incorporating geochemical changes into design, such as conducting sensitivity analyses and implementing relevant monitoring tools.

2.5.1. Sensitivity Analyses

As mentioned in the previous sections, tailings are likely to undergo changes to their material properties throughout the lifetime of the TSF. By conducting sensitivity analyses, tailings engineers can evaluate the susceptibility of their structure to failure given changes in geotechnical parameters such as particle size, porosity, void ratio, consolidation, plasticity, permeability, etc. These are all parameters with cause for concern given the literature review summarized in this chapter; however, the answer is still unclear as to exactly how and to what extent these parameters will change and, as such, legacy facilities with similar mineralogy and composition should be evaluated at depth to observe impacts of weathering on specific geotechnical parameters. If adequate laboratory standards were developed that could capture these complex transformations, this would be recommended as a tool to predict material property changes. These parameter ranges could then be inserted into a geotechnical slope stability software and/or dam breach analysis to determine the sensitivity of the structure to material property changes.

2.5.2. Monitoring Tools

Monitoring relevant phenomena that are indicative of geochemical processes is another option for observing the rate of transformation and predicting material changes. Recommendations for in-situ and/or remote monitoring tools are summarized below and categorized based on failure mode.

2.5.2.a. Monitoring Flow-Type Stability Failure Modes

Monitoring flow-type stability failures (i.e., brittle behavior) is not an easy task. Historically, brittle behavior has been observed post-liquefaction, occurring so rapidly

there is no time for mitigation. A summary of geochemical and geotechnical parameters to monitor for and potential monitoring tools are presented below:

- Changes in mineralogy: As in the case of Brumadinho, remolded specimens from the embankment had > 50% iron content (Robertson et al., 2019).
- Surface precipitation (as an indicator of changes in mineralogy): iron oxidation visible on the surface may be detectable via satellite imagery, visual observation, and infrared (IR) spectroscopy (e.g., drone).
- Settlement: Slowed consolidation or settlement due to rigid structure observed via horizontal inclinometers or settlement gauges. ‘Slowed’ may be relative to rates calculated via laboratory consolidation tests performed on new (non-weathered) specimens.
- Geochemical parameters (where measurable) (e.g., paste pH, ORP, $\text{CO}_{2(g)}$ concentrations, temp.): to inform speciation of secondary minerals and if subsequent changes in tailings structure increase potential for brittle behavior. For example, goethite has a hardness of 5-5.5 on the Mohs hardness scale which contributes to a rigid soil skeleton, whereas jarosite has a hardness of 2.5-3.5 and thus a less rigid soil skeleton (Mukherjee, 2012; Ng et al., 2019).
- Phreatic surface and/or moisture content: many cementitious materials are also soluble in water. Therefore, observing surface moisture content via remote sensing and/or in-situ sensors is important to ensuring minerals will not dissolve and collapse the soil fabric. Monitoring phreatic surface via piezometers is useful for delineation of the phreatic surface.

2.5.2.b. Monitoring Water Management Failure Modes

Water management is one of the most common TSF failure modes (Davies et al., 2002). The following list includes recommendations for monitoring changes in water management induced specifically by geochemical processes.

- Pond size: decreased particle size, increased water retention capacity, lowered hydraulic conductivity, and pipe clogging can all lead to hindered drainage. Observing pond size and location via satellite imagery and drone footage can inform potential pond locations that are unfavorable, such as pond encroachment of the embankment as reported in Jagersfontein post-failure analysis (Torres-Cruz and O'Donovan, 2023)
- Phreatic surface: pipe clogging, formation of hardpans, and/or generation of fines can lead to a rise in the phreatic surface. The phreatic surface can be monitored via piezometers.
- Degree of oxidation at depth: see Questa Rock Pile Weathering and Stability Project for more information. Borehole samples analyzed for mineralogy, paste pH, moisture content, acid-base accounting, leach extraction, forward acid titration testing, grain size analysis, moisture retention, and permeability. In-situ testing of temperature, O_{2(g)}, and CO_{2(g)} concentrations in boreholes as an indicator of degree and rate of oxidation and microbial activity (Robertson, 2001; URS Corporation, 2001; Shaw et al., 2002). Multi-level microbial analysis may also inform in situ zonation.
- Surface precipitation: secondary mineral formation can be detected on the surface of the TSF and be an indicator of weathering. Iron oxides and hardpans

are typically orange in color, whereas gypsum formation and calcite precipitation are white/yellow in color (Bryant, 2005). This can be observed via satellite imagery (Sentinel-2) if in-situ data of paste pH and mineralogy are available to calibrate results.

- **Settlement:** formation of secondary minerals can reduce self-weight consolidation due to lower density and less inter-particle void space. Detectable via deviations in field behavior, measured via horizontal inclinometers or settlement gauges, or remote sensing methods (e.g., InSAR, LiDAR), relative to settlement predicted from models calibrated with lab tests run on new tailings specimens.

2.5.2.c. Monitoring Internal Erosion and Piping Failure Modes

Two-thirds of internal erosion and piping failures occur within the first 5 years of operation (Fell et al., 2015). Piping is visually detectable once mass loss or seepage has already occurred in the embankment; however, the goal would be to detect signs indicative of internal erosion and piping before they occur. The following list summarizes potential monitoring tools:

- **Seepage water quality:** alkaline or basic seepage waters can be indicative of carbonate mineral dissolution (Ca^{2+} and Mg^{2+} ions released due to dissolution, H^+ ions consumed).
- **Pore water chemistry:** acidic seepage directly upstream of the embankment can result in soluble mineral dissolution within the dam.
- **$\text{CO}_2(\text{g})$ concentrations:** carbonate dissolution leads to high partial pressures of carbon dioxide gas in TSF pore water relative to atmospheric conditions ($10^{-3.5}$

bar at sea level). Monitoring CO₂ within TSF and foundational materials can help detect internal erosion failures, whereas monitoring CO₂ in the embankment can help detect piping failures.

- Surface observations: visual observations of changes in moisture content, particle size, and erosion can be interpreted via satellite imagery (Section 4.2).
- Settlement: localized deformations due to mass loss via carbonate dissolution can be detected via remote sensing methods (e.g., InSAR, LiDAR, or with settlement gauges).

2.5.2.d. Monitoring Foundational Failure Modes

Various foundational failure modes can and have occurred; however, this thesis focuses specifically on those exasperated by geochemical processes. The following list summarizes recommendations for in-situ monitoring.

- Settlement: vertical deformation can be indicative of karstic bedrock dissolution, as well as sulfide-induced heave (gypsum formation). Measured via horizontal inclinometers or settlement gauges (Fell et al., 2015), or remote sensing methods (e.g., InSAR, LiDAR).
- Permeability: the increase or decrease in permeability of the foundation can be detected by changes to the phreatic surface within the TSF, and/or adjacent groundwater. High-permeability foundations resulting from soluble mineral dissolution will result in a drop in internal phreatic surface (and potentially increased levels of adjacent groundwater), whereas low permeability foundation due to soluble mineral precipitation can lead to a rise in the internal phreatic surface (and a reduction in adjacent groundwater levels as the intensity of the

TSF sources is reduced). Water levels may be monitored by piezometers located at various depths within the TSF.

- Groundwater flow rates: monitoring for potential changes in groundwater flow rates can also be representative of changes to foundation permeability. A decrease in groundwater flow either due to pore clogging or to avoid mixing contact water with non-contact water can lead to supersaturation of minerals and subsequent precipitation.
- Groundwater quality: measurement of upstream and downstream water quality in terms of pH, mineral content, ORP, EC, etc. can guide inferences related to soluble mineral dissolution/precipitation reactions occurring within the foundation. Monitoring wells should already be located upstream and downstream of the TSF.
- Seepage quality: Seepage water quality can guide predictions on modifications to foundation. Acidic seepage could lead to soluble mineral dissolution (i.e., karstic bedrock), sulfide-induced heave (i.e., gypsum formation), transformation of silicates to phyllosilicates (clay), and/or alteration of clay properties (DDL, flocculation, etc.).
- Geochemical parameters: monitoring temperature, $O_{2(g)}$ and $CO_{2(g)}$ concentrations at various depths in the foundation can help inform understanding of the degree and location of oxidation and microbial activity. Monitoring $CO_{2(g)}$ levels is especially important for ensuring safety, as seen in the case of Carsington Dam (Section 2.4.4).

Overall, monitoring relevant phenomena related to geochemical transformations of legacy and operating TSFs needs to be implemented on a global scale to gain more insight about the evolution of TSFs under various geological and environmental conditions and to provide more insight into mitigating potential failure modes. New and developing technologies are discussed in Chapter 4 which makes monitoring at a global scale more practical.

CHAPTER 3. LABORATORY METHODS & PRELIMINARY RESULTS

3.1. Objectives and Hypotheses

While many mineralogical and physical analyses have been conducted on weathered tailings, there are no standard laboratory methods for studying the influence of geochemical weathering on geotechnical properties such as hydraulic conductivity, consolidation, shear strength, etc. This study was designed to analyze one of the many geochemical processes discussed in Chapter 2, calcite dissolution (2b), due to chemical simplicity and high solubility under acidic conditions and subsequent influence on geotechnical parameters upon dissolution. The chemical equation for calcite dissolution is as follows:



This study serves as a “proof of concept” and was designed with the intent of monitoring geochemical changes with inlayed pH and ORP (redox) sensors to predict live changes in geochemistry and, subsequently, geotechnical properties. Mineral phases can be distinguished with information gathered from pH and ORP sensors and, as such, inferences on the geotechnical properties (strength, hardness, permeability, compressibility, etc.) can be made. Due to the inaccessibility of sensors within the time frame of this project, the pH, redox, and electrical conductivity (EC) were monitored at the influent and effluent until geochemical equilibrium was achieved. Unfortunately, geochemical equilibrium was not achieved within the four-week time frame of this experiment and the columns will continue to permeate until geochemical equilibrium is achieved with results to be published later.

Our hypothesis for this experiment was that calcite dissolution would lead to an increase in hydraulic conductivity due to mass loss, internal erosion, and/or piping. Assuming that calcite is completely dissolved upon termination, a decrease in effective stress would be anticipated due to an increase in void space, less particle interlocking, and a looser fabric which is contractive upon loading. Hydraulic conductivity would be anticipated to increase as mineral dissolution creates preferential flow paths. Consolidation should increase due to a higher void ratio. If calcite were to reprecipitate in the columns at neutral pH values, the inverse effect would be expected on the values of geotechnical parameters (i.e., an increase in shear strength due to aggregate formation/light cementation, a decrease in hydraulic conductivity, and a decrease in consolidation).

3.2. Methods and Materials

Fine synthetic tailings (FST) were used to control the physical and chemical properties of the columns. The FST followed the specifications as prepared by Hamade and Bareither (2019), consisting of 40% kaolin (Thiele Kaolin Company, Sandersville, GA) and 60% silica flour (U.S. Silica Holdings Inc., Frederick, MD). All columns were prepared with deionized (DI) water. The geotechnical properties of the FST, as determined by Hamade & Bareither (2019) are presented in Table 1. In the columns with calcite, 10% (by mass) calcite replaced equal parts of kaolin and silica sand. Calcite was obtained from Fisher Scientific and has a specific gravity (G_s) of 2.71 g/cm^3 .

Table 1: Summary of fine synthetic tailings geotechnical characteristics. Unified Soil Classification System (USCS) soil type is lean clay (CL).

Material	FST
Liquid Limit (LL) (%)	37
Plasticity Index (PI) (%)	15
USCS	CL
G_s	2.63
d_{max} (mm)	0.05
Gravel Content (%)	0
Sand Content (%)	0
Fines Content (%)	100
Clay Content (%)	42
γ_{dmax} (kN/m ³)	14.9

The columns were 25.4 cm tall and 10.2 cm wide to accommodate for the depth required for a laboratory vane shear (2x the height of the vane); however, this height-to-diameter ratio exceeds the recommended ratio of 0.4 to avoid the side-wall effect under consolidation, and wider columns should be used if the experiment were to be repeated (ASTM D2435). The slurry was prepared at a solids content of 25% and mixed at an average rate of 600 rpm for 3 minutes, to achieve full suspension of the particles. The slurry was poured into the columns and allowed to settle until there was no visible deformation.

A Seepage-Induced Consolidation Test (SICT) method was used to measure both hydraulic conductivity and consolidation under applied hydraulic gradients (Tian et al., 2019). Due to the large surface area of the inflow compared to the smaller surface area of the effluent, a constant head rising tailwater hydraulic conductivity test was used. The

following equation was used to get an initial hydraulic conductivity assuming a uniform void ratio at depth (later corrected via large-strain consolidation theory).

$$k = \frac{\Delta V * L}{A * \Delta h * \Delta t} \quad (\text{Equation 2})$$

Three consolidation steps were implemented (1 kPa, 10 kPa, and 50 kPa), with settlement measurements taken simultaneously along with hydraulic conductivity readings. The termination criteria for the non-geochemically altered columns (1, 2, 3, and 4) was achieving four consecutive measurements of hydraulic conductivity within $\pm 25\%$ of the average hydraulic conductivity. Termination criteria for the geochemically altered columns (5, 6, 7, and 8) was reaching chemical equilibrium, or equivalent values of influent and effluent pH. Finally, the shear strength was measured using the Wille Geotechnik mini vane shear apparatus (electrical transducer) with a vane diameter and height of 12.7 mm and 25.4 mm, respectively. The blade thickness and shaft diameter were 0.8 mm and 3 mm, respectively. The vane was rotated at a rate of 6°/min and after a vane insertion duration time of 2 minutes (ASTM D4648; Biscontin & Pestana, 2001; Islam, 2020). After determination of undrained shear strength, a water content sample was collected according to ASTM D2216. A summary of all the column experiments is presented in Table 2.

Table 2: Summary of all column experiment inputs

Column	Mixture	Permeant Water
1	FST – Control	DI water
2	FST – Control	DI water
3	FST – Calcite	DI water
4	FST – Calcite	DI water
5	FST – Calcite	Dilute Nitric Acid (pH \approx 3.0)
6	FST – Calcite	Dilute Nitric Acid (pH \approx 3.0)
7	FST – Calcite	Dilute Sodium Hydroxide (pH \approx 10)
8	FST – Calcite	Dilute Sodium Hydroxide (pH \approx 10)
9	FST – Control	Dilute Nitric Acid (pH \approx 3.0)
10	FST – Control	Dilute Nitric Acid (pH \approx 3.0)
11	FST – Control	Dilute Sodium Hydroxide (pH \approx 10)
12	FST – Control	Dilute Sodium Hydroxide (pH \approx 10)

3.3. Data Analysis

Large-strain consolidation theory developed by Gibson et al., (1967) was used to overcome the limitation of small-strain consolidation theory which assumes constant material properties during consolidation (Terzaghi, 1936). Slurry-deposited materials are known to vary in compressibility and hydraulic conductivity during consolidation as a function of effective stress and, as such, are more suitable for large-strain consolidation theory (Koppula, 1970; Carrier et al., 1983; Abu-Hejleh et al., 1996; Fox and Berles, 1997). Large-strain consolidation theory operates under the assumptions that (i) the soil skeleton is homogenous, and creep does not occur during consolidation; (ii) soil solids and fluid are incompressible; and (iii) the principle of effective stress is valid. Therefore, Equation 3 is the result of combining the governing equation for large strain consolidation theory with the principle of Terzaghi’s effective stress equation (Znidarčić et al., 1992).

$$\sigma'(z) = \sigma'_0 + \int_0^z (\gamma_s - \gamma_w) dz + \int_0^z \frac{V_D \gamma_w}{k} (1 + e) dz \quad (\text{Equation 3})$$

where γ_w = unit weight of water, γ_s = unit weight of solid particles, V_D = Darcy's seepage velocity, k = hydraulic conductivity, and e = void ratio. The first two terms on the right-hand side of the equation reflect the applied surface stress (in this case, $\sigma'_0 = 0$ kPa), and the self-weight consolidation of the specimen at depth, whereas the last term reflects the seepage force (Tian et al., 2019). Based on this governing relationship, constitutive relationships were developed between (i) void ratio and effective stress and (ii) hydraulic conductivity and void ratio (Liu and Znidarčić, 1991; Znidarčić et al., 1992; Gjerapic et al., 2008).

$$e = A * (\sigma' + Z)^B \quad (\text{Equation 4})$$

$$k = C * e^D \quad (\text{Equation 5})$$

Finally, iterative procedures were conducted based on Tian et al. (2019). The constitutive relationships in Equations 4-5 were solved to yield Equations 6-8 as a function of the empirical parameters B and D.

$$A = \frac{e_0}{Z^B} \quad (\text{Equation 6})$$

$$Z = \frac{\sigma'}{\left(\frac{e}{e_0}\right)^{1/B} - 1} \quad (\text{Equation 7})$$

$$C = \frac{k}{(e)^D} \quad (\text{Equation 8})$$

3.4. Preliminary Results

Table 3 summarizes all empirical parameters for columns 1, 2, and 4.

Table 3: Summary of empirical parameters (Z, A, C, B, and D) for columns 1, 2, and 4.

Column	Z	A	C	B	D
1	3.08	3.43	0.00	-0.28	11.60
2	110.8	4.3×10^{10}	0.00	-5.00	0.10
4	0.337	2.11	1.89×10^{-9}	-0.05	5.61

Figure 16 shows laboratory results for vertical deformation over time for columns 1, 2, and 4. Columns 1 and 2 are duplicates consisting of FST (no calcite) mixed with deionized water and should have similar trends (albeit varying parameters). Columns 3 and 4 consist of FST (w/ calcite) mixed with deionized water; however, due to a piping failure, column 3 failed before termination (Appendix A) and the remaining column tests are ongoing.

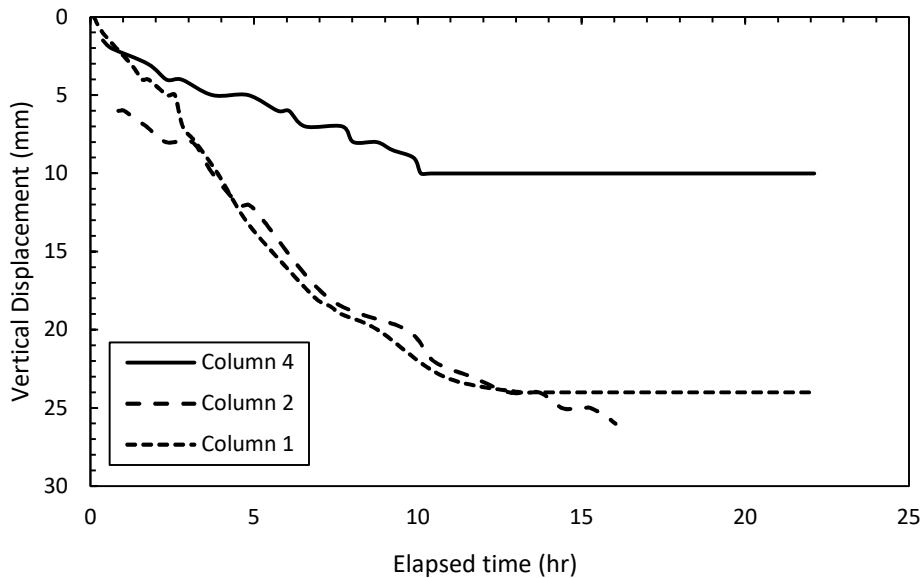


Figure 16: Relationship between vertical displacement (mm) and elapsed time (hr) for columns 1, 2, and 4.

Plots of void ratio versus effective stress and void ratio versus hydraulic conductivity for columns 1, 2, and 4, are presented in Figures 17 and 18, respectively. “Data” represents laboratory data gathered whereas, “fit” represents the curve-fitting power functions based on the large-strain consolidation theory and the parameters summarized in Table 3.

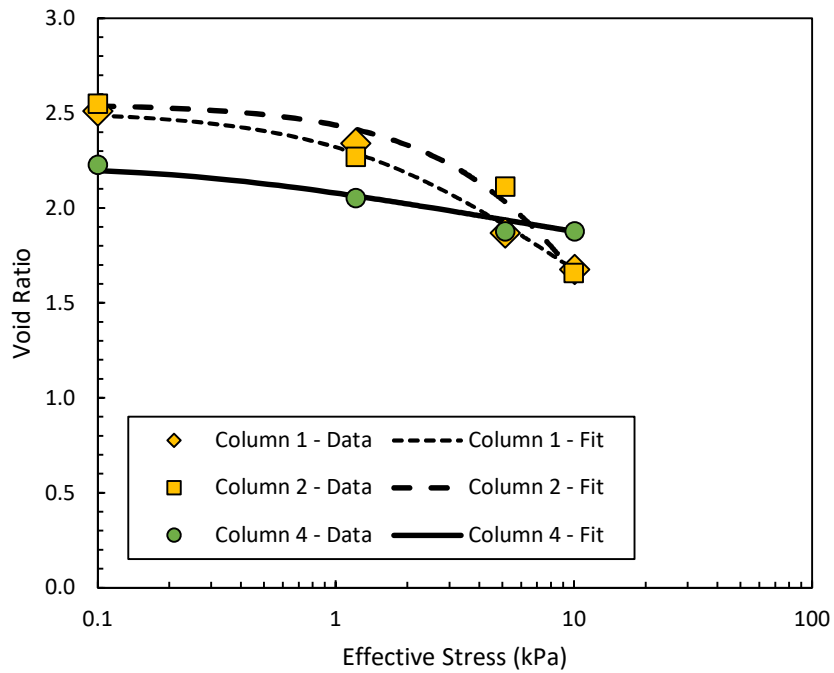


Figure 17: Relationship between final void ratio and effective stress (kPa) for columns 1, 2, and 4.

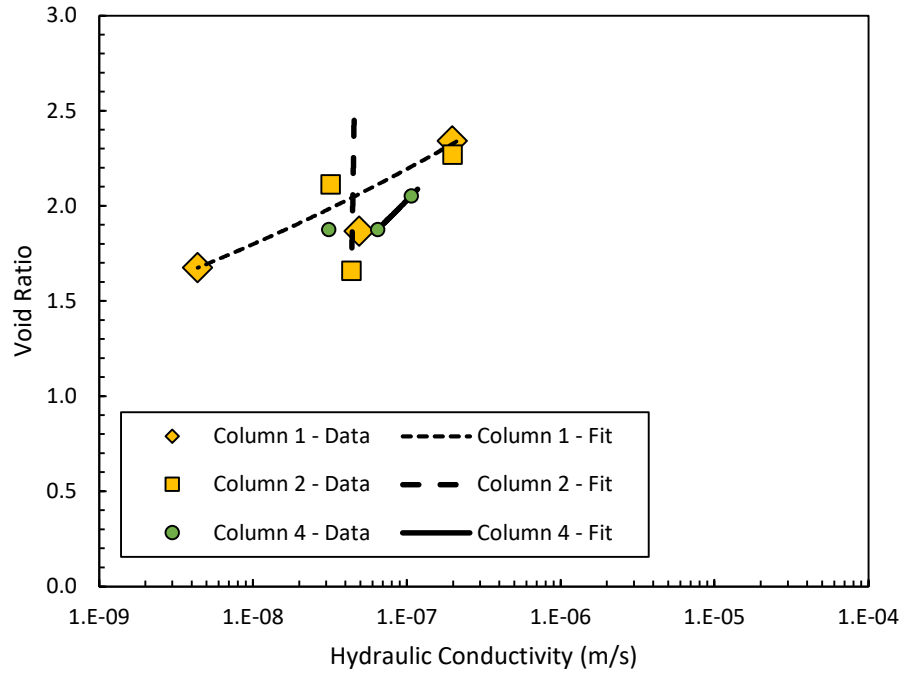


Figure 18: Relationship between final void ratio and hydraulic conductivity (m/s) for columns 1, 2, and 4.

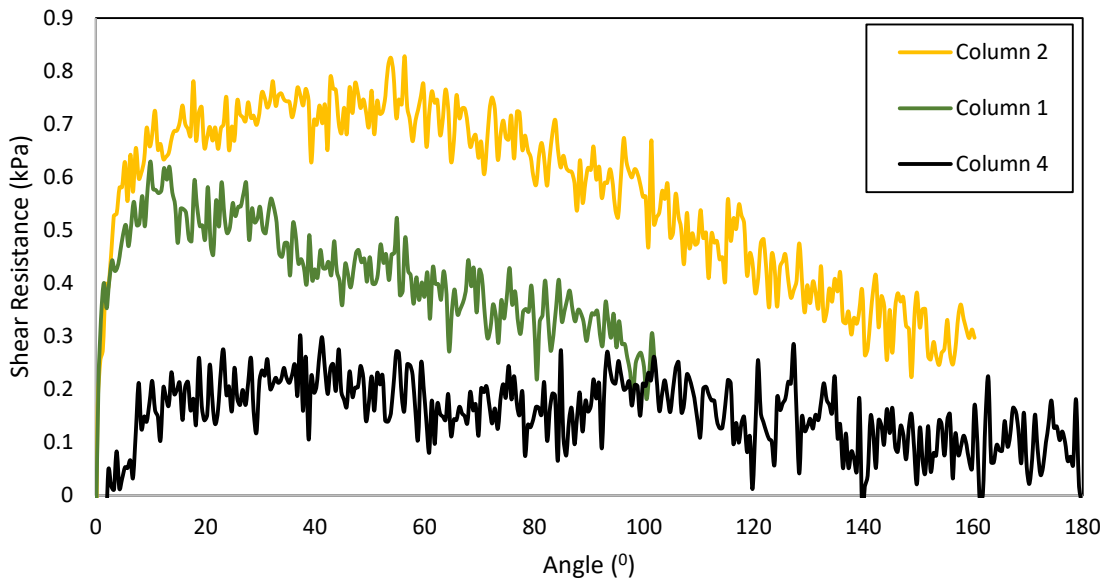


Figure 19: Results of laboratory mini vane shear for columns 1, 2, and 4.

The preliminary results are inconsistent with the expected outcomes. Reduced settlement and low compressibility of column 4 relative to columns 1 and 2 would be consistent with the idea that calcite dissolution is occurring and precipitates are forming at grain contacts, thus forming a rigid soil skeleton. Conversely, no significant difference in hydraulic conductivity is observed as would be expected with calcite dissolution, and the shear strength of column 4 is lower than for columns 1 and 2, signifying a weaker material (no cementation). This may be due to the disturbance of grain-to-grain contacts upon insertion of the vane shear; however, being that no observations were made at the microscale, and there was no significant fluctuation in effluent geochemical parameters, a conclusion regarding the mechanisms taking place within the column and subsequent influence on geotechnical stability cannot be made.

CHAPTER 4. FUTURE WORK AND CONCLUSIONS

4.1. Questa Rock Pile Weathering and Stability Project

The Questa Rock Pile Weathering and Stability Project, sponsored by Chevron Mining Inc., is one of the most extensive, multi-disciplinary studies evaluating the impacts of physical and chemical weathering on the geotechnical stability of pyritic rock piles. Mining activity took place in the town of Questa, New Mexico from 1965-1983, in which 74 million tons of low-grade molybdenum ore was mined. The Questa mine site consists of 9 waste rock piles, containing a total of 320 million tons, and with an estimated 2-3% pyrite volumetrically based on concentrations in the surrounding vein zones (Shaw et al., 2002). Signs of visible weathering are present in the nearby hydrothermal scars (local steep slopes, lack of vegetation, discoloration, etc.) and gypsum and jarosite formation on the surface of the waste rock piles. Following a shallow foundational failure in the underlying sheared colluvium and signs of creep in the Goat Hill North Rock Pile, regrading took place in 2005 to reduce the load on the foundation and reinforce the toe of the rock pile with placement of a buttress (Norwest Corporation, 2003, 2004).

The regrading of the rock pile presented a unique opportunity to evaluate the degree of weathering at depth and address concerns regarding long-term stability. A 250-ft borehole allowed for the analysis of oxygen and carbon dioxide levels at depth, as well as temperature, to predict the current state of oxidation. Depleted oxygen levels at the surface due to iron and sulfide oxidation, high CO₂ levels at the surface due to gypsum and jarosite formation, and high oxygen levels within the rock pile implied that weathering had occurred and that there is future potential for ongoing weathering at depth (Shaw et al., 2002). Elevated temperatures with increasing depth were also observed, due in part to

microbial activity and/or exothermic reactions (Shaw et al., 2002). The borehole was also analyzed via the following geochemical and physical testing: moisture content, acid-base accounting (ABA), paste pH, leach extraction, forward acid titration testing, grain size distribution, and permeability (Robertson, 2001; Shaw et al., 2002; URS Corporation, 2001). Other geotechnical tests conducted on split samples from trench sampling include direct shear, point load strength, slake durability tests, Atterberg limits, and particle size distribution (Gutierrez et al., 2008).

Overall, the rate of feldspar hydrolysis, clay formation, and subsequent decrease in friction angle was determined to be at a rate slow enough to be deemed inconsequential (Gutierrez et al., 2008; McLemore & van Zyl, 2008; URS Corporation, 2001). The main takeaway, however, is not what this report says for this one facility. As many practicing geologists and engineers will tell you, there is no “blueprint” approach for tailings storage facilities, and no environmental, mineralogical, and geological setting will be the same for multiple facilities. The relevance of this study is that extensive geochemical and geotechnical characterization of the rock pile was conducted during mandatory regrading of a legacy mine landform. If timed correctly, these types of studies can provide invaluable data to further our understanding of the topic and, to my knowledge, no similar report in breadth and scale has been generated for a TSF.

4.2. Remote Sensing

Remote sensing is “the science of remotely acquiring, processing, and interpreting spectral information about the Earth’s surface that records interactions between matter and electromagnetic energy” (Sabins, 1997). The ability to remotely acquire data provides a new opportunity in the mining industry, as remote technologies can provide records of sites

where information was previously lacking. For example, a recent case study on the Jagersfontein dam failure in South Africa used publicly available satellite imagery to determine that the construction sequence of the dam did not align with safe and reliable tailings management practices (Torres-Cruz and O'Donovan, 2023). The authors used images from the Sentinel-2 satellite which has been capturing open-source data since 2015 with 13 bands in visible and near infrared light (VNIR) region at a resolution of 10 m/pixel (European Space Agency, 2015; Van der Werff and Van der Meer, 2015). Sentinel-2 images have also been applied in a geochemical context, to monitor and track ARD (Seifi et al., 2018; Soydan et al., 2020) and to identify secondary mineral formation in waste rock piles (Hauff et al., 2013). Crowley et al., (2003) studied the spectral reflectance properties of 15 Fe-bearing minerals in the VNIR region.

An important caveat to remote sensing techniques is that field data are often needed to corroborate results (i.e., paste pH, mineralogy, etc.). An example from the Questa rock pile, Goat Hill North, is shown in Figures 19 and 20 in which iron oxide and clay mineral formation was observed via hyperspectral remote sensing techniques (Hauff et al., 2013).

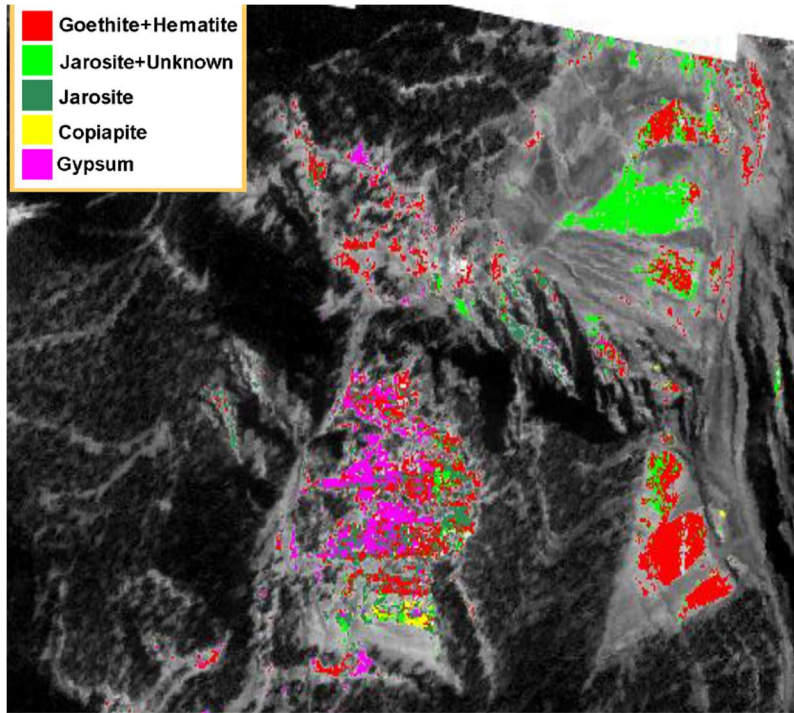


Figure 20: Results of remote-sensing imagery on the Goat Hill North rock pile showing visible goethite, hematite, jarosite, copiapite, and gypsum surface precipitation (from Hauff et al., 2013).

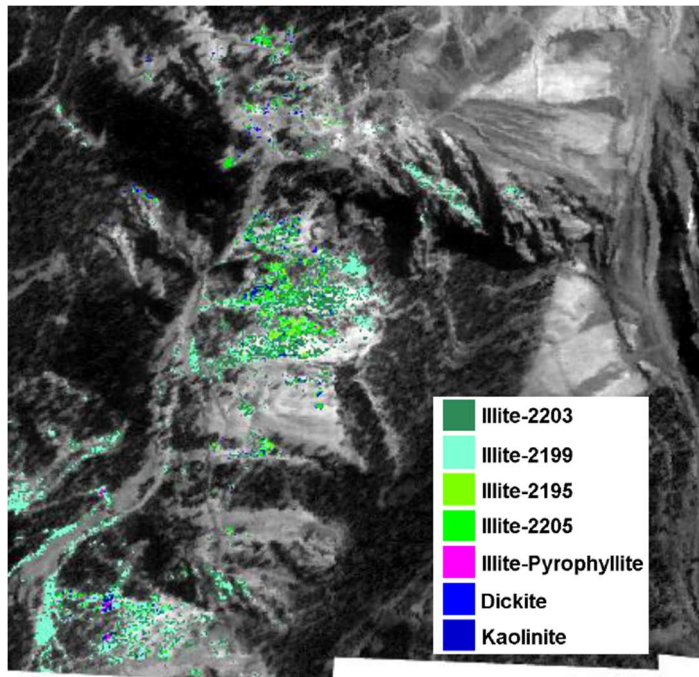


Figure 21: Results of remote-sensing imagery on the Goat Hill North rock pile showing surficial clay formation from weathered silicates (from Hauff et al., 2013).

Real-time monitoring of pH, redox, conductivity, and temperature could be a solution to gathering spatiotemporal in-situ data needed for calibrating remote sensing techniques. Advanced, multi-parameter, cloud-based sensors have been extensively studied and implemented by the groundwater contaminant hydrology field to monitor the natural attenuation of hydrocarbons (Blotevogel et al., 2021; Sale et al., 2020).

Land subsidence can be quantified using remote sensing techniques such as LiDAR (Light Detection and Ranging) and/or InSAR (Interferometric Synthetic Aperture Radar). LiDAR has been used by the mining industry to evaluate erosion of legacy facilities (Martín-Velázquez et al., 2022), generate maps of active deformation (Hu et al., 2023), monitor consolidation settlement (Hu et al., 2017), and more. A recent study by Vulpe et al., (2022) used InSAR data to monitor changes in tailings settlement and swelling behavior following variations in weather patterns and seepage flow.

Given the volume change behavior of some secondary mineral precipitates (gypsum, jarosite, goethite, etc.) and anticipated mass loss due to soluble mineral dissolution, various weathering stages of a TSF could be observed via Sentinel-2 imaging and correlated to deformation via LiDAR and/or InSAR imaging. Future work should use public domain tools, such as Google Earth Engine, to combine deformation data and Sentinel- 2 imaging and create maps which can be used to understand current and predict future settlement and volume change properties in correspondence with weathering reactions. In addition, the placement of real-time monitoring sensors at depth would allow for monitoring of the oxidation front within a tailings deposit, tracking of geochemical evolution of the structure over time, and important data collection needed for remote sensing techniques.

Furthermore, as remote sensing data evolves to higher resolutions, remote imaging will be

able to track geotechnical parameters such as particle size, moisture content, gradation, etc. that are known to be indicators of slope stability and piping failures – serving as another preventative tool. Overall, the future development of high-resolution, hyper-spectral imaging is going to open a new window of opportunity in monitoring the geochemical evolution of TSFs that is more efficient and robust than traditional monitoring techniques.

4.3. Future Field and Laboratory Methods

Ng et al. (2019) conducted a critical state analysis on lateritic soils (high content of aluminum and iron oxides) and similar studies should be conducted on weathered tailings to observe changes in the critical state line, compressibility, friction angle, etc. In addition, Cone Penetration Testing (CPT) is the industry standard for in-situ testing; however, to my knowledge, there are no calibration parameters for weakly cementitious soils. Similarly, there is no guidance on conducting seismicity studies on weakly cemented soils (Vucetic M, 1992, Clarkson and Williams, 2021).

Potential mine waste management strategies are also being explored, including 1) commingling, showing promising results in terms of reducing sulfide oxidation (slowing weathering) and promoting geotechnical stability, and 2) changes to ore processing techniques, producing a more geochemically and geomechanically stable tailings (finer particles are more reactive and prone to failure) (Wilson, 2022; Pearce, 2022). Overall, tailings professionals are actively coming up with unique solutions to this problem and should continue sharing solutions whenever possible to advance the current state of practice.

4.4. Microbial Technologies

Microbes have been explored for their utility in “eco-engineering” of tailings which promote root vegetation via increased organic carbon sequestration, particle aggregation, and neutralization of alkaline tailings (Yi et al., 2023; Yi *et al.*, 2021; Trippe et al., 2021; Wu et al., 2019). Other important uses of microbes in tailings include bioaugmentation to promote hardpan formation for cover placement (Liu et al., 2021), bioleaching (Henne et al., 2018), and microbially induced calcite precipitation to cement tailings (Mujah et al., 2017). Overall, microbes have great potential for future studies given that their contribution to weathering rates have yet to be accounted for in design and predictive modeling. Microbial technologies are extremely cost-efficient and low-energy and I believe they will continue to prove their favorability over traditional engineering solutions in the coming years.

4.5. Conclusion

Overall, the goal from this work is for tailings engineers to be more familiar with the geochemical processes occurring with a TSF and to be more prepared for monitoring and detecting geochemically induced failure modes before they occur, as well as conducting post-failure analyses with coupled geochemical considerations in mind. Incorporation of predictive modeling of geochemical processes and their subsequent impacts on geotechnical stability should also be incorporated into modern practice. Logsdon (2022) suggests a reasonable mine closure planning period of 200 – 500 years based on time scales seen in effective management of low-level nuclear wastes and an expected geological and hydrogeological data collection period of 100 years (50 years operational, 50 years active closure and reclamation). In addition, a semi-quantitative assessment should be conducted

which determines whether major changes in performance are expected within 500 and 1,000 years (Logsdon, 2022). This is based on observations of active oxidation of pyrite occurring along hydrothermal scars that have been exposed for 30,000 to 1.5 million years in Questa, NM (Logsdon, 2011).

Lastly, my hope is that this document and embedded conceptual models may be used as a tool for tailings engineers to use in client conversations to elaborate on the importance of in-depth geochemical characterization of tailings before operations and placement begins, as well as in the design of facilities and establishment of monitoring protocols.

REFERENCES

- Agnew, M., & Taylor, G. F. (2000). Development, cycling and effectiveness of hardpans and cemented layers in tailings storage facilities in Australia. *Australian Workshop on Acid Mine Drainage. Townsville, Australia*, 157–169.
- Ahmed, S. M. (1995). Chemistry of pyrrhotite hardpan formation. *Conference on Mining and the Environment, 1*, 171–180.
- Alakangas, L., & Öhlander, B. (2006). Formation and composition of cemented layers in low-sulphide mine tailings, Laver, northern Sweden. *Environmental Geology*, 50(6), 809–819. <https://doi.org/10.1007/s00254-006-0253-x>
- ASTM International. (2020). *Standard Test Methods for One-Dimensional Consolidation Properties of Soils Using Incremental Loading*.
https://compass.astm.org/document/?contentCode=ASTM%7CD2435_D2435M-11R20%7Cen-US
- ASTM International. (2016). *Standard Test Methods for Laboratory Miniature Vane Shear Test for Saturated Fine-Grained Clayey Soil*.
https://compass.astm.org/document/?contentCode=ASTM%7CD4648_D4648M-16%7Cen-US
- ASTM International. (2019). *Standard Test Methods for Laboratory Determination of Water (Moisture) Content of Soil and Rock by Mass*.
<https://compass.astm.org/document/?contentCode=ASTM%7CD2216-19%7Cen-US>
- Balkenhol, R., Ludwig, B., Ufer, K., Jochum, J., & Friedrich, G. (2001). Pyrite oxidation in sediment samples from the German open-cut brown coal mine Zwenkau: Mineral

formation and dissolution of silicates. *Journal of Plant Nutrition and Soil Science*, 164(3), 283–288. [https://doi.org/10.1002/1522-2624\(200106\)164:3<283::AID-JPLN283>3.0.CO;2-4](https://doi.org/10.1002/1522-2624(200106)164:3<283::AID-JPLN283>3.0.CO;2-4)

Biscontin, G., & Pestana, J. (2001). Influence of Peripheral Velocity on Vane Shear Strength of an Artificial Clay. *Geotechnical Testing Journal*, 24(4), 423. <https://doi.org/10.1520/GTJ11140J>

Blight, G. E. (2010). *Geotechnical Engineering for Mine Waste Storage Facilities*. Taylor & Francis Group, London, UK.

Blotevogel, J., Karimi Askarani, K., Hanson, A., Gallo, S., Carling, B., Mowder, C., Spain, J., Hartten, A., & Sale, T. (2021). Real-Time Remediation Performance Monitoring with ORP Sensors. *Groundwater Monitoring & Remediation*, 41(3), 27–28. <https://doi.org/10.1111/gwmr.12479>

Blowes, D. W., Jambor, J. L., Hanton-Fong, C. J., Lortie, L., & Gould, W. D. (1998). Geochemical, mineralogical and microbiological characterization of a sulphide-bearing carbonate-rich gold-mine tailings impoundment, Joutel, Québec. *Applied Geochemistry*, 13(6), 687–705. [https://doi.org/10.1016/S0883-2927\(98\)00009-2](https://doi.org/10.1016/S0883-2927(98)00009-2)

Blowes, D. W., Reardon, E. J., Jambor, J. L., & Cherry, J. A. (1991). The formation and potential importance of cemented layers in inactive sulfide mine tailings. *Geochimica et Cosmochimica Acta*, 55(4), 965–978. [https://doi.org/10.1016/0016-7037\(91\)90155-X](https://doi.org/10.1016/0016-7037(91)90155-X)

- Blowes, D. W., & Jambor, J. L. (1990). The pore-water geochemistry and the mineralogy of the vadose zone of sulfide tailings, Waite Amulet, Quebec, Canada. *Applied Geochemistry*, 5(3), 327–346. [https://doi.org/10.1016/0883-2927\(90\)90008-S](https://doi.org/10.1016/0883-2927(90)90008-S)
- Bryant, L. (2003). *Geotechnical Problems with Pyritic Rock and Soil*. Virginia Polytechnic Institute and State University.
- Cambridge, M. (Ed.). (2018). *The Hydraulic Transport and Storage of Extractive Waste*. Springer International Publishing. <https://doi.org/10.1007/978-3-319-69248-7>
- Carelsen, S. (2013). *Influence of capillary bridges on weathered tailings material*. University of Twente. <https://essay.utwente.nl/84632/1/carelsen.pdf>
- Carrier, W. D., Bromwell, L. G., & Somogyi, F. (1983). Design Capacity of Slurried Mineral Waste Ponds. *Journal of Geotechnical Engineering*, 109(5), 699–716. [https://doi.org/10.1061/\(ASCE\)0733-9410\(1983\)109:5\(699\)](https://doi.org/10.1061/(ASCE)0733-9410(1983)109:5(699))
- Casey, J., Friedel, R., & Chambers, R. (2022). Characterizing Tailings Behavior at the San Manuel Copper TSFs Part 1: In-situ and Laboratory Geotechnical Techniques. *Tailings and Mine Waste Conference '22*.
- Clarkson, L., & Williams, D. (2021). An Overview of Conventional Tailings Dam Geotechnical Failure Mechanisms. *Mining, Metallurgy & Exploration*, 38(3), 1305–1328. <https://doi.org/10.1007/s42461-021-00381-3>
- Crowley, J. K., Williams, D. E., Hammarstrom, J. M., Piatak, N., Chou, I.-M., & Mars, J. C. (2003). Spectral reflectance properties (0.4–2.5 μm) of secondary Fe-oxide, Fe-hydroxide, and Fe-sulphate-hydrate minerals associated with sulphide-bearing mine

wastes. *Geochemistry: Exploration, Environment, Analysis*, 3(3), 219–228.

<https://doi.org/10.1144/1467-7873/03-001>

Davies, M. P., McRoberts, E., & Martin, T. (2002). Static liquefaction of tailings— fundamentals and case histories. *Proceedings Tailings Dams ASDSO/USCOLD*.

DeSisto, S. L., Jamieson, H. E., & Parsons, M. B. (2011). Influence of hardpan layers on arsenic mobility in historical gold mine tailings. *Applied Geochemistry*, 26(12), 2004–2018. <https://doi.org/10.1016/j.apgeochem.2011.06.030>

Devasahayam, S. (2006). Chemistry of acid production in black coal mine washery wastes. *International Journal of Mineral Processing*, 79(1), 1–8.

<https://doi.org/10.1016/j.minpro.2005.11.004>

Dultz, S. (2002). Effects of parent material and weathering on feldspar content in different particle size fractions from forest soils in NW Germany. *Geoderma*, 106(1–2), 63–81.

[https://doi.org/10.1016/S0016-7061\(01\)00116-1](https://doi.org/10.1016/S0016-7061(01)00116-1)

Duncan, J. M., Wright, S. G., & Brandon, T. L. (2014). *Soil Strength and Slope Stability*. John Wiley & Sons, Incorporated.

<http://ebookcentral.proquest.com/lib/csu/detail.action?docID=1767444>

Durocher, J., Robertson, L., & Usher, B. (2017). Sulfide Oxidation in Tailings Storage Facilities: An Influence to Long Term Dam Stability. *Tailings and Mine Waste '17*.

Durocher, J., Robertson, L., & Usher, B. (2022). Geochemical interactions and long-term dam stability: An update. *Tailings and Mine Waste Conference '22*.

Elghali, A., Benzaazoua, M., Bouzahzah, H., Abdelmoula, M., Dynes, J. J., & Jamieson, H. E. (2021). Role of secondary minerals in the acid generating potential of weathered

mine tailings: Crystal-chemistry characterization and closed mine site management involvement. *Science of The Total Environment*, 784, 147105.

<https://doi.org/10.1016/j.scitotenv.2021.147105>

Elghali, A., Benzaazoua, M., Bussière, B., Kennedy, C., Parwani, R., & Graham, S. (2019). The role of hardpan formation on the reactivity of sulfidic mine tailings: A case study at Joutel mine (Québec). *Science of The Total Environment*, 654, 118–128.

<https://doi.org/10.1016/j.scitotenv.2018.11.066>

European Space Agency. (2015). *Sentinel User Handbook and Exploitation Tools (SUHET): Sentinel-2 User Handbook* (Issue 1 Rev. 2). European Commission.

Evangelou, V. P. (Bill), & Zhang, Y. L. (1995). A review: Pyrite oxidation mechanisms and acid mine drainage prevention. *Critical Reviews in Environmental Science and Technology*, 25(2), 141–199. <https://doi.org/10.1080/10643389509388477>

Fell, R., MacGregor, P., Stapledon, D., Bell, G., & Foster, M. (2015). *Geotechnical Engineering of Dams* (2nd ed.). CRC Press.

Filipowicz, P., & Borys, M. (2007). Comparative analysis of the geotechnical properties of coal mining wastes from Lublin Coal Basin and from other basins. *Journal of Water and Land Development*, 11(1). <https://doi.org/10.2478/v10025-008-0010-5>

Flemming, H.-C. (2011). The perfect slime. *Colloids and Surfaces B: Biointerfaces*, 86(2), 251–259. <https://doi.org/10.1016/j.colsurfb.2011.04.025>

Forsberg, L. S., & Ledin, S. (2002). *Effects of Iron Precipitation and Organic Amendments on Porosity and Penetrability in Sulphide Mine Tailings*. 14.

- Fox, P. J., & Berles, J. D. (1997). CS2: A Piecewise-Linear Model for Large Strain Consolidation. *International Journal for Numerical and Analytical Methods in Geomechanics*, 21(7), 453–475. [https://doi.org/10.1002/\(SICI\)1096-9853\(199707\)21:7<453::AID-NAG887>3.0.CO;2-B](https://doi.org/10.1002/(SICI)1096-9853(199707)21:7<453::AID-NAG887>3.0.CO;2-B)
- Gens, A., & Alonso, E. E. (2006). Aznalcóllar dam failure. Part 2: Stability conditions and failure mechanism. *Géotechnique*, 56(3), 185–201. <https://doi.org/10.1680/geot.2006.56.3.185>
- Gibson, R. E., Schiffman, R. L., & Cargill, K. W. (1981). The theory of one-dimensional consolidation of saturated clays. II. Finite nonlinear consolidation of thick homogeneous layers. *Canadian Geotechnical Journal*, 18(2), 280–293. <https://doi.org/10.1139/t81-030>
- Gjerapic, G., Johnson, J., Coffin, J., & Znidarcic, D. (2008). Determination of Tailings Impoundment Capacity via Finite-Strain Consolidation Models. *GeoCongress 2008*, 798–805. [https://doi.org/10.1061/40972\(311\)99](https://doi.org/10.1061/40972(311)99)
- Gleeson, K., Newcombe, G., Griffin, P., & Stephenson, P. (2020). *Cadia Operations, New South Wales, Australia, NI 43-101 Technical Report*. Newcrest Mining Limited.
- Gratchev, I., & Towhata, I. (2013). Stress–strain characteristics of two natural soils subjected to long-term acidic contamination. *Soils and Foundations*, 53(3), 469–476. <https://doi.org/10.1016/j.sandf.2013.04.008>
- Gutierrez, L. A. F., Viterbo, V. C., McLemore, V. T., & Aimone-Martin, C. T. (2008). Geotechnical and Geomechanical Characterisation of the Goathill North Rock Pile at the Questa Molybdenum Mine, New Mexico, USA. *Rock Dumps 2008: Proceedings of*

the First International Seminar on the Management of Rock Dumps, Stockpiles and Heap Leach Pads, Australian Centre for Geomechanics, 19–32.

https://doi.org/10.36487/ACG_repo/802_2

Hamade, M. M. P., & Bareither, C. A. (2019). *Consolidated Undrained Shear Behavior of Synthetic Waste Rock and Synthetic Tailings Mixtures*.

<https://compass.astm.org/document/?contentCode=ASTM%7CGTJ20180007%7Cen-US&proxycl=https%3A%2F%2Fsecure.astm.org&fromLogin=true>

Hauff, P. L., Peters, D. C., Coulter, D. W., & Prosh, E. C. (2013). *Presence of Clays and Weathering at the Questa Mine, New Mexico*.

Hawkins, A. B., & Pinches, G. M. (1997). Understanding sulphate generated heave resulting from pyrite degradation. *Ground Chemistry Implications for Construction: Proceedings of the International Conference on the Implications of Ground Chemistry and Microbiology for Construction.*, 51-75.

Henne, A., Craw, D., Vasconcelos, P., & Southam, G. (2018). Bioleaching of waste material from the Salobo mine, Brazil: Recovery of refractory copper from Cu hosted in silicate minerals. *Chemical Geology*, 498, 72–82.

<https://doi.org/10.1016/j.chemgeo.2018.08.029>

Hu, L., Tomás, R., Tang, X., López Vinielles, J., Herrera, G., Li, T., & Liu, Z. (2023).

Updating Active Deformation Inventory Maps in Mining Areas by Integrating InSAR and LiDAR Datasets. *Remote Sensing*, 15(4), 996. <https://doi.org/10.3390/rs15040996>

Hu, X., Oommen, T., Lu, Z., Wang, T., & Kim, J.-W. (2017). Consolidation settlement of Salt Lake County tailings impoundment revealed by time-series InSAR observations

from multiple radar satellites. *Remote Sensing of Environment*, 202, 199–209.

<https://doi.org/10.1016/j.rse.2017.05.023>

International Commission on Large Dams (ICOLD). (2001). *Tailings dams. Transport. Placement. Decantation. Review and recommendations.*

Islam, S., Williams, D. J., Llano-Serna, M., & Zhang, C. (2020, May 2). *Settling, consolidation and shear strength behaviour of coal tailings slurry* | Elsevier Enhanced Reader. <https://doi.org/10.1016/j.ijmst.2020.03.013>

Koppula, S. D. (1970). *The Consolidation of Soil in Two Dimensions and with Moving Boundaries.* University of Alberta (Canada).

Kotzer, T., Sexsmith, K., Chambers, R., Casey, J., & Friedel, R. (2022). Characterizing Tailings Behavior at the San Manuel Copper TSFs Part 2: Imaging Techniques at Tailings-Matrix Scale. *Tailings and Mine Waste Conference '22.*

Lin, Z. (1997). Mobilization and retention of heavy metals in mill-tailings from Garpenberg sulfide mines, Sweden. *Science of The Total Environment*, 198(1), 13–31. [https://doi.org/10.1016/S0048-9697\(97\)05433-8](https://doi.org/10.1016/S0048-9697(97)05433-8)

Liu, J., & Znidarčić, D. (1991). Modeling One-Dimensional Compression Characteristics of Soils. *Journal of Geotechnical Engineering*, 117(1), 162–169. [https://doi.org/10.1061/\(ASCE\)0733-9410\(1991\)117:1\(162\)](https://doi.org/10.1061/(ASCE)0733-9410(1991)117:1(162))

Liu, Y., Wu, S., Nguyen, T. A. H., Southam, G., Chan, T.-S., Lu, Y.-R., & Huang, L. (2018). Microstructural characteristics of naturally formed hardpan capping sulfidic copper-lead-zinc tailings. *Environmental Pollution*, 242, 1500–1509. <https://doi.org/10.1016/j.envpol.2018.08.027>

Liu, Y., Wu, S., Southam, G., Chan, T.-S., Lu, Y.-R., Paterson, D. J., & Huang, L. (2021).

Bioaugmentation with *Acidithiobacillus* species accelerates mineral weathering and formation of secondary mineral cements for hardpan development in sulfidic Pb-Zn tailings. *Journal of Hazardous Materials*, 411, 124988.

<https://doi.org/10.1016/j.jhazmat.2020.124988>

Liu, Y., Wu, S., Southam, G., Nguyen, T. A. H., Kopittke, P. M., Paterson, D. J., & Huang,

L. (2019). Zinc and lead encapsulated in amorphous ferric cements within hardpans in situ formed from sulfidic Cu-Pb-Zn tailings. *Environmental Pollution*, 252, 1106–

1116. <https://doi.org/10.1016/j.envpol.2019.06.069>

Logsdon, M. (2011) Questa Weathering and Stability Study: Geological, Hydrogeological, and Geochemical Framework. Tailings and Mine Waste '11, November 5-9,

Vancouver BC.

Logsdon, M. (2022). *Say what you mean and mean what you say: Determining the period-of-performance for managing reactive, sulfide-bearing mine wastes*. 12th International Conference on Acid Rock Drainage, Virtual (Australia).

Lottermoser, B. G., & Ashley, P. M. (2006). Mobility and retention of trace elements in hardpan-cemented cassiterite tailings, north Queensland, Australia. *Environmental Geology*, 50(6), 835–846. <https://doi.org/10.1007/s00254-006-0255-8>

Martín-Velázquez, S., Rodríguez-Santalla, I., Roperó-Szymańska, N., Gomez-Ortiz, D.,

Martín-Crespo, T., & De Ignacio-San José, C. (2022). Geomorphological Mapping and Erosion of Abandoned Tailings in the Hiendelaencina Mining District (Spain) from

Aerial Imagery and LiDAR Data. *Remote Sensing*, 14(18), 4617.

<https://doi.org/10.3390/rs14184617>

McBride, M. B. (1994). *Environmental Chemistry of Soils*. Oxford University Press.

McGregor, R. G., & Blowes, D. W. (2002). The physical, chemical and mineralogical properties of three cemented layers within sulfide-bearing mine tailings. *Journal of Geochemical Exploration*, 76(3), 195–207. [https://doi.org/10.1016/S0375-6742\(02\)00255-8](https://doi.org/10.1016/S0375-6742(02)00255-8)

McGregor, R. G., Blowes, D. W., Jambor, J. L., & Robertson, W. D. (1998). The solid-phase controls on the mobility of heavy metals at the Copper Cliff tailings area, Sudbury, Ontario, Canada. *Journal of Contaminant Hydrology*, 33(3–4), 247–271. [https://doi.org/10.1016/S0169-7722\(98\)00060-6](https://doi.org/10.1016/S0169-7722(98)00060-6)

McLemore, V. T., & van Zyl, D. (2009). *Extrapolation of Geotechnical and Geochemistry Characterization into the Future* (DRA-51; Questa Weathering Study, pp. 1–17).

Mitchell, J. K., & Soga, K. (2005). *Fundamentals of Soil Behavior* (3rd ed.). John Wiley & Sons.

Morkeh, J., & McLemore, V. T. (2012). *The effect of particle size fractions on chemistry, mineralogy, and acid potential of the Questa Rock Piles, Taos County, New Mexico* (Open-File Report No. 545).

Mujah, D., Shahin, M. A., & Cheng, L. (2017). State-of-the-Art Review of Biocementation by Microbially Induced Calcite Precipitation (MICP) for Soil Stabilization. *Geomicrobiology Journal*, 34(6), 524–537. <https://doi.org/10.1080/01490451.2016.1225866>

- Mukherjee, S. (2011). *Applied Mineralogy*. Springer Netherlands.
<https://doi.org/10.1007/978-94-007-1162-4>
- Ng, C. W. W., Akinniyi, D. B., Zhou, C., & Chiu, C. F. (2019). Comparisons of weathered lateritic, granitic and volcanic soils: Compressibility and shear strength. *Engineering Geology*, 249, 235–240. <https://doi.org/10.1016/j.enggeo.2018.12.029>
- Nordstrom, D. (2003). Effects of microbiological and geochemical interactions in mine drainage. *Environmental Aspects of Mine Wastes*, 31, 227–238.
- Nordstrom, D. K., Blowes, D. W., & Ptacek, C. J. (2015). Hydrogeochemistry and microbiology of mine drainage: An update. *Applied Geochemistry*, 57, 3–16.
<https://doi.org/10.1016/j.apgeochem.2015.02.008>
- Nordstrom, D. K., & Southam, G. (1997). Geomicrobiology of Sulfide Mineral Oxidation. *Geomicrobiology: Interactions between Microbes and Minerals*, 35, 361–391.
- Norwest Corporation. (2003). *Goathill North mine rock pile evaluation and conceptual mitigation plan*. Unpublished Report to Molycorp Inc (p. 56).
- Norwest Corporation. (2004). *Goathill North slide investigation, evaluation and mitigation report*, Unpublished Report to Molycorp Inc. (p. 94).
- Otieno, F., & Shukla, S. K. (2022). An insight into failure of iron ore mine tailings dams. *International Journal of Mining, Reclamation and Environment*, 1–21.
<https://doi.org/10.1080/17480930.2022.2159295>
- Pearce, S., McCann, P., Mueller, S., Brookshaw, D. (2022). *Optimization of process flow and metallurgy to reduce risks from acid and metalliferous drainage in tailings and recover critical metals*. 12th International Conference on Acid Rock Drainage, Virtual (Australia).

- Perez-Lopez, R., Nieto, J. M., Alvarez-Valero, A. M., & De Almodovar, G. R. (2007). Mineralogy of the hardpan formation processes in the interface between sulfide-rich sludge and fly ash: Applications for acid mine drainage mitigation. *American Mineralogist*, 92(11–12), 1966–1977. <https://doi.org/10.2138/am.2007.2686>
- Power, I. M., Paulo, C., Long, H., Lockhart, J. A., Stubbs, A. R., French, D., & Caldwell, R. (2021). Carbonation, Cementation, and Stabilization of Ultramafic Mine Tailings. *Environmental Science & Technology*, 55(14), 10056–10066. <https://doi.org/10.1021/acs.est.1c01570>
- Rico, M., Benito, G., Salgueiro, A. R., Díez-Herrero, A., & Pereira, H. G. (2008). Reported tailings dam failures. *Journal of Hazardous Materials*, 152(2), 846–852. <https://doi.org/10.1016/j.jhazmat.2007.07.050>
- Ridley, J. (2023). “Ore Deposit Geochemistry: Lecture Notes”. Colorado State University, Fort Collins, CO.
- Robertson, A. M. (2001). *Weathering of Hydrothermally Altered Sulfide Mine Rock and the Potential for Slope Failures at Questa Mine, New Mexico*. Robertson Geoconsultants, Inc.
- Robertson, P. K., de Melo, L., Williams, D. J., & Wilson, G. W. (2019). *Report of the Expert Panel on the Technical Causes of the Failure of Feijão Dam I*. 81.
- Rowe, R. K., Armstrong, M. D., & Cullimore, D. R. (2000). Particle Size and Clogging of Granular Media Permeated with Leachate. *Journal of Geotechnical and Geoenvironmental Engineering*, 126(9), 775–786. [https://doi.org/10.1061/\(ASCE\)1090-0241\(2000\)126:9\(775\)](https://doi.org/10.1061/(ASCE)1090-0241(2000)126:9(775))

- Sabins, F. F. (1997). *Remote Sensing. Principles and Interpretation* (3rd ed.). W. H. Freeman & Co.
- Sale, T., Gallo, S., Askarani, K. K., Irianni-Renno, M., Lyverse, M., Hopkins, H., Blotevogel, J., & Burge, S. (2021). Real-time soil and groundwater monitoring via spatial and temporal resolution of biogeochemical potentials. *Journal of Hazardous Materials*, 408, 124403. <https://doi.org/10.1016/j.jhazmat.2020.124403>
- Schippers, A., Breuker, A., Blazejak, A., Bosecker, K., Kock, D., & Wright, T. L. (2010). The biogeochemistry and microbiology of sulfidic mine waste and bioleaching dumps and heaps, and novel Fe(II)-oxidizing bacteria. *Hydrometallurgy*, 104(3–4), 342–350. <https://doi.org/10.1016/j.hydromet.2010.01.012>
- Seedsman, R. W., & Emerson, W. W. (1985). The role of clay-rich rocks in spoil pile failures at Goonyella Mine, Queensland, Australia. *International Journal of Rock Mechanics and Mining Sciences & Geomechanics Abstracts*, 22(2), 113–118. [https://doi.org/10.1016/0148-9062\(85\)92333-2](https://doi.org/10.1016/0148-9062(85)92333-2)
- Seifi, A., Hosseinjanizadeh, M., Ranjbar, H., & Honarmand, M. (2019). Identification of Acid Mine Drainage Potential Using Sentinel 2a Imagery and Field Data. *Mine Water and the Environment*, 38(4), 707–717. <https://doi.org/10.1007/s10230-019-00632-2>
- Shaw, S., Wels, C., Robertson, A., & Lorinczi, G. (2002). Physical and Geochemical Characterization of Mine Rock Piles at the Questa Mine, New Mexico, An Overview. *Tailings & Mine Waste '02 Conference*. Tailings & Mine Waste '02 Conference, Fort Collins, CO.

- Singer, P. C., & Stumm, W. (1970). Acidic Mine Drainage: The Rate-Determining Step. *Science*, *167*(3921), 1121–1123.
- Soydan, H., Koz, A., & Düzgün, H. Ş. (2021). Secondary Iron Mineral Detection via Hyperspectral Unmixing Analysis with Sentinel-2 Imagery. *International Journal of Applied Earth Observation and Geoinformation*, *101*, 102343.
<https://doi.org/10.1016/j.jag.2021.102343>
- Spagnoli, G., Rubinos, D., Stanjek, H., Fernández-Steeger, T., Feinendegen, M., & Azzam, R. (2012). Undrained shear strength of clays as modified by pH variations. *Bulletin of Engineering Geology and the Environment*, *71*(1), 135–148.
<https://doi.org/10.1007/s10064-011-0372-9>
- Stucki, J. W., Goodman, B. A., & Schwertmann, U. (Eds.). (1987). *Iron in Soils and Clay Minerals*. Springer Netherlands. <https://doi.org/10.1007/978-94-009-4007-9>
- Terzaghi, K. (1936). The shearing resistance of saturated soils and the angle between the planes of shear. *1st International Conference on Soil Mechanics and Foundation Engineering*, *1*, 54–56.
- Tian, Z., Bareither, C. A., & Scalia, J. (2019). *Development and Assessment of a Seepage-Induced Consolidation Test Apparatus*. <https://doi.org/10.1520/GTJ20180375>
- Torres-Cruz, L. A., & O'Donovan, C. (2023). Public remotely sensed data raise concerns about history of failed Jagersfontein dam. *Scientific Reports*, *13*(1), 4953.
<https://doi.org/10.1038/s41598-023-31633-5>
- Trippe, K. M., Manning, V. A., Reardon, C. L., Klein, A. M., Weidman, C., Ducey, T. F., Novak, J. M., Watts, D. W., Rushmiller, H., Spokas, K. A., Ippolito, J. A., & Johnson,

- M. G. (2021). Phytostabilization of acidic mine tailings with biochar, biosolids, lime, and locally-sourced microbial inoculum: Do amendment mixtures influence plant growth, tailing chemistry, and microbial composition? *Applied Soil Ecology*, 165, 103962. <https://doi.org/10.1016/j.apsoil.2021.103962>
- URS Corporation. (2001). *Mine rock pile erosion and stability evaluations, Questa mine, Unpublished Report to Molycorp, Inc.*
- U.S. Bureau of Reclamation (USBR). (2019). *Internal Erosion Risks For Embankments And Foundations* (Best Practice and Risk Methodology, Security, Safety, and Law Enforcement Office – Dam Safety).
<https://usbr.gov/ssle/damsafety/risk/BestPractices/Chapters/D6-InternalErosionRisksForEmbankmentsAndFoundationsWithAppendices.pdf>
- Van Der Werff, H., & Van Der Meer, F. (2015). Sentinel-2 for Mapping Iron Absorption Feature Parameters. *Remote Sensing*, 7(10), 12635–12653.
<https://doi.org/10.3390/rs71012635>
- Vick, S. G. (1990). *Planning, design, and analysis of tailings dams*. BiTech Publishers Ltd.
<http://hdl.handle.net/2429/76455>
- Vucetic, M. (1992). Soil properties and seismic response. *Proceedings of the 10th World Conference of Earthquake Engineering*, 1199–1204.
https://www.iitk.ac.in/nicee/wcee/article/10_vol3_1199.pdf
- Vulpe, C., Fourie, A., Gavin, R., Magnall, N., Larkin, H., Thomas, A., McNab, L., & Boshoff, J. (2022). *Monitoring the effect of weather on settlement response of tailings by means of InSAR*. Tailings and Mine Waste Conference '22, Denver, Colorado.

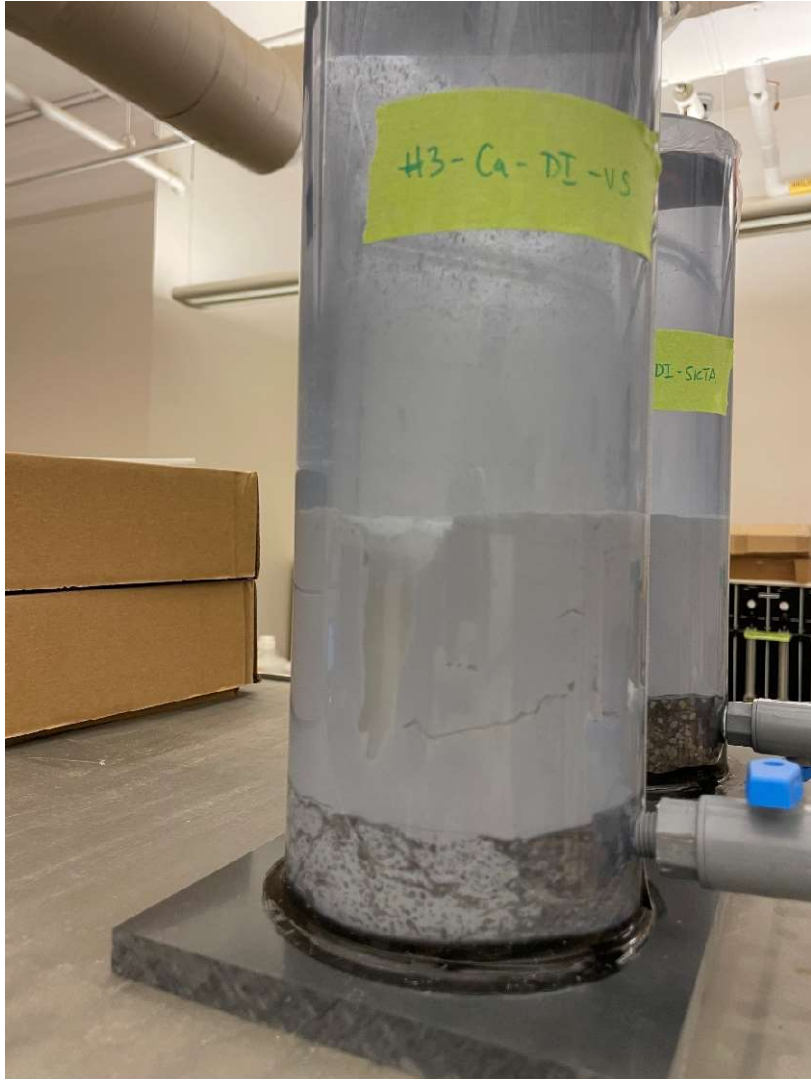
- Wang, C., Harbottle, D., Liu, Q., & Xu, Z. (2014). Current state of fine mineral tailings treatment: A critical review on theory and practice. *Minerals Engineering*, 58, 113–131. <https://doi.org/10.1016/j.mineng.2014.01.018>
- Wang, G., Liu, X., Song, L., Ma, X., Chen, W., & Qiao, J. (2023). Micro-structure and morphology of tailings sand under different oxidation and acidification degree. *Scientific Reports*, 13(1), Article 1. <https://doi.org/10.1038/s41598-022-26130-0>
- Wilson, W. (2022). *Producing geochemical and physical stability in mine waste deposits – the big picture: Case studies in commingling – Part I*. 12th International Conference on Acid Rock Drainage, Virtual (Australia).
- WISE Uranium Project. (2015). *The Los Frailes tailings dam failure (Aznalcóllar, Spain)*. <https://www.wise-uranium.org/mdaflf.html>
- Wu, J., Wu, Y., & Lu, J. (2008). Laboratory study of the clogging process and factors affecting clogging in a tailings dam. *Environmental Geology*, 54(5), 1067–1074. <https://doi.org/10.1007/s00254-007-0873-9>
- Wu, J., Wu, Y., Lu, J., & Lee, L. (2007). Field investigations and laboratory simulation of clogging in Lixi tailings dam of Jinduicheng, China. *Environmental Geology*, 53(2), 387–397. <https://doi.org/10.1007/s00254-007-0654-5>
- Wu, S., Liu, Y., Southam, G., Robertson, L., Chiu, T. H., Cross, A. T., Dixon, K. W., Stevens, J. C., Zhong, H., Chan, T.-S., Lu, Y.-J., & Huang, L. (2019). Geochemical and mineralogical constraints in iron ore tailings limit soil formation for direct phytostabilization. *Science of The Total Environment*, 651, 192–202. <https://doi.org/10.1016/j.scitotenv.2018.09.171>

- Yamanaka, T., Miyasaka, H., Aso, I., Tanigawa, M., Shoji, K., & Yohta, H. (2002). Involvement of Sulfur- and Iron-Transforming Bacteria in Heaving of House Foundations. *Geomicrobiology Journal*, 19(5), 519–528. <https://doi.org/10.1080/01490450290098487>
- Yi, Q., Wu, S., Liu, Y., Chan, T.-S., Lu, Y.-R., Saha, N., Southam, G., & Huang, L. (2023). Mineral weathering of iron ore tailings primed by *Acidithiobacillus ferrooxidans* and elemental sulfur under contrasting pH conditions. *Science of The Total Environment*, 856, 159078. <https://doi.org/10.1016/j.scitotenv.2022.159078>
- Yi, Q., Wu, S., Southam, G., Robertson, L., You, F., Liu, Y., Wang, S., Saha, N., Webb, R., Wykes, J., Chan, T.-S., Lu, Y.-R., & Huang, L. (2021). Acidophilic Iron- and Sulfur-Oxidizing Bacteria, *Acidithiobacillus ferrooxidans*, Drives Alkaline pH Neutralization and Mineral Weathering in Fe Ore Tailings. *Environmental Science & Technology*, 55(12), 8020–8034. <https://doi.org/10.1021/acs.est.1c00848>
- Zhang, C., Ma, C., Xiong, J., & Jiang, Q. (2022). Tailings Dam Geotechnical Stability Improvement due to Flocculants Treated Fine Tailings Dewatering. *Geotechnical and Geological Engineering*. <https://doi.org/10.1007/s10706-022-02300-9>
- Znidarčić, D., Abu-Hejleh, A. N., & Barnes, B. L. (1996). Consolidation Characteristics of Phosphatic Clays. *Journal of Geotechnical Engineering*, 122(4), 295–301. [https://doi.org/10.1061/\(ASCE\)0733-9410\(1996\)122:4\(295\)](https://doi.org/10.1061/(ASCE)0733-9410(1996)122:4(295))

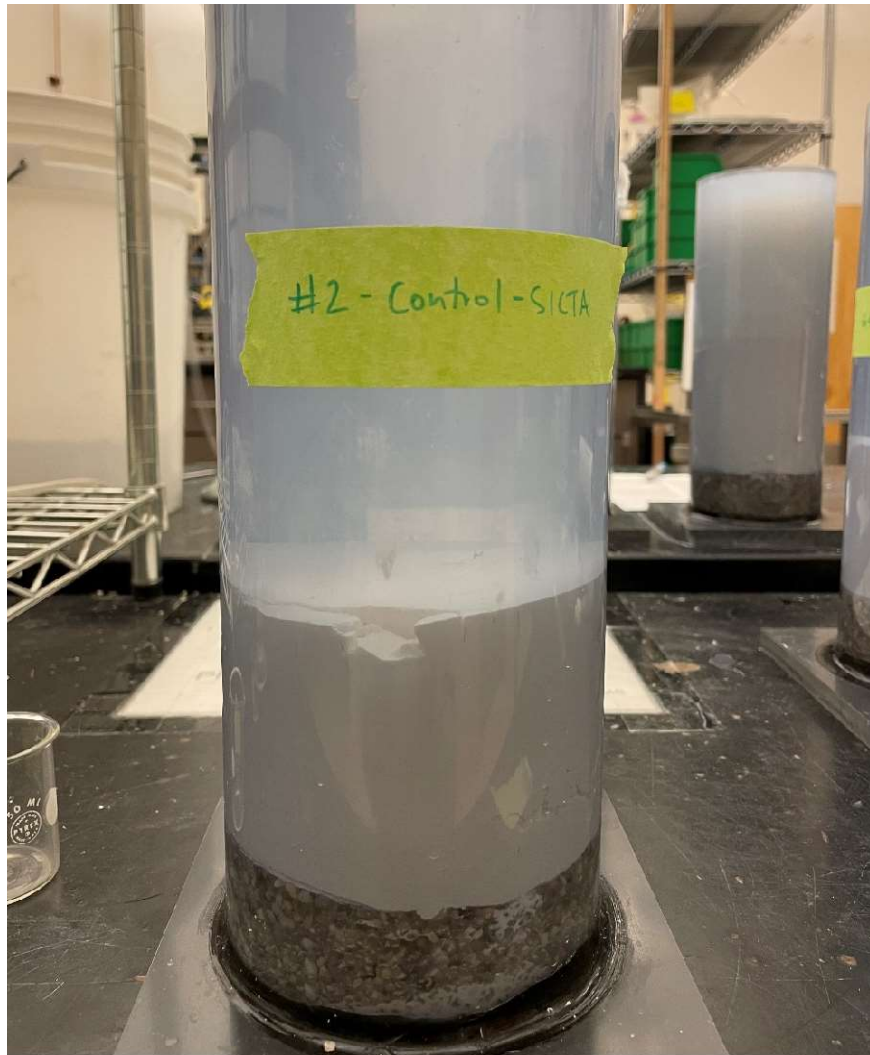
APPENDIX A. LABORATORY PHOTOS



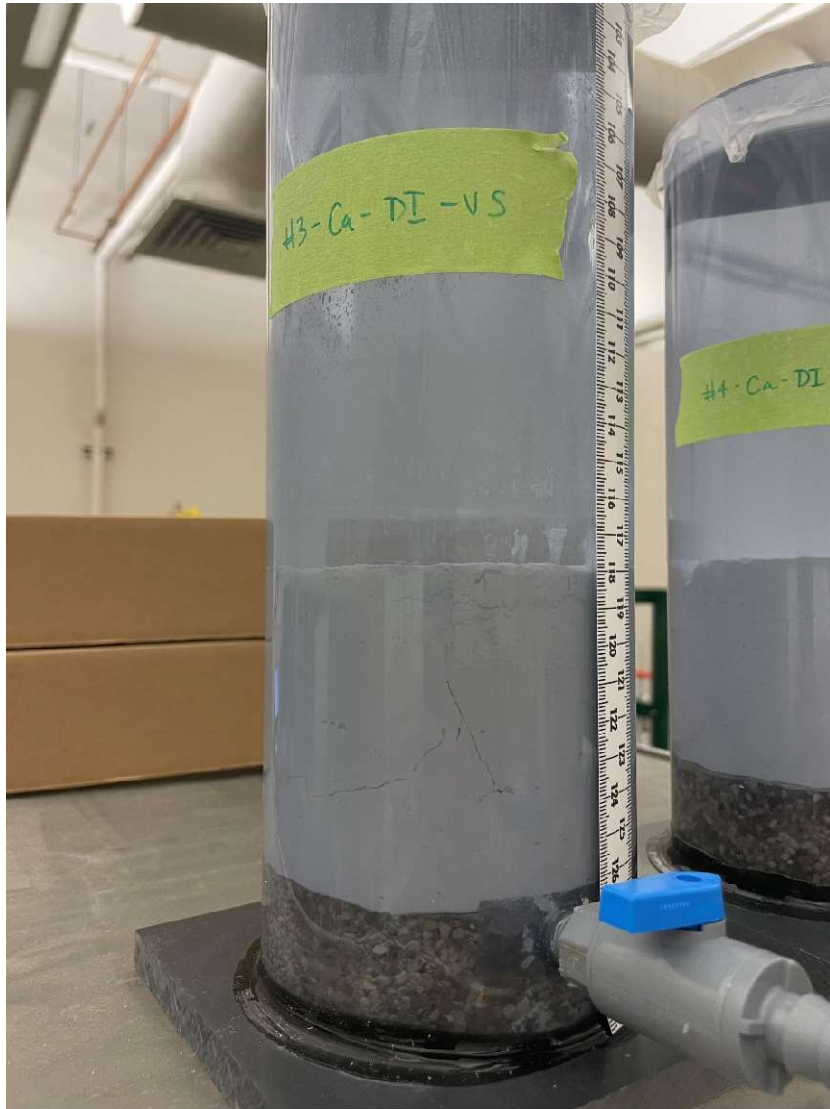
A1: Photo of all column experiments.



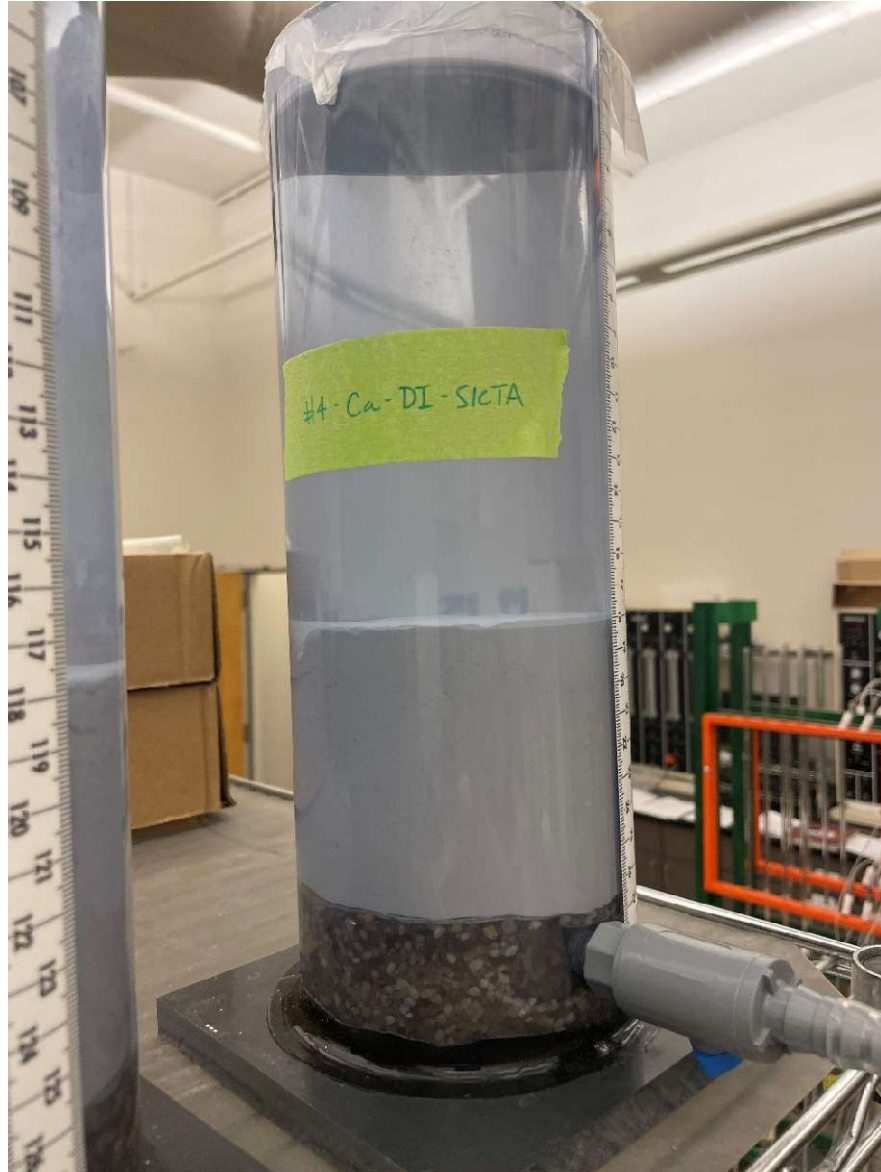
A2: Example of "piping" failure seen in Column 3.



A3: Image of Column 2 with slight deformation on the surface.



A4: Image of cracks forming in Column 3 prior to failure.



A5: Image of Column 4 showing no visible deformation or failure.